NASA TECHNICAL NOTE

NASA TN D-7846

NASA TN D-7846

RELIABILITY APPROACH TO ROTATING-COMPONENT DESIGN

Dimitri B. Kececioglu and Vincent R. Lalli

Lewis Research Center

Cleveland, Ohio 44135

NATIONAL AERONAUTICS AND SPACE ADMINISTRATION • WASHINGTON, D. C. • FEBRUARY 1975

1. Report No.	2. Government Accession No.	3. Recipient's Catalog No.
NASA TN D-7846		

4. Title and Subtitle	5. Report Date
RELIABILITY APPROACH TO ROTATING-COMPONENT DESIGN	February 1975
	6. Performing Organization Code

7. Author(s)	8. Performing Organization Report No.
Dimitri B. Kececioglu, University of Arizona, Tucson, Arizona, and Vincent R. Lalli, Lewis Research Center	E-5528
	10. Work Unit No. 120-60

9. Performing Organization Name and Address	11. Contract or Grant No.
Lewis Research Center National Aeronautics and Space Administration Cleveland, Ohio 44135	

12. Sponsoring Agency Name and Address	13. Type of Report and Period Covered
National Aeronautics and Space Administration Washington, D. C. 20546	Technical Note
	14. Sponsoring Agency Code

15. Supplementary Notes

16. Abstract

A probabilistic methodology for designing rotating mechanical components using reliability to relate stress to strength is explained. The experimental test machines and data obtained for steel to verify this methodology are described. A sample mechanical rotating component design problem is solved by comparing a deterministic design method with the new design-by reliability approach. The new method shows that a smaller size and weight can be obtained for a specified rotating shaft life and reliability. The new methodology uses the statistical distortion-energy theory with statistical fatigue diagrams for optimum shaft design. Other mechanical components can be designed as well with this methodology. Statistical methods applied to design problems can lead to new goals of realism in engineering design. Designers should recognize that the deterministic design method is a special case of the more general design-by-reliability approach.

17. Key Words (Suggested by Author(s))	18. Distribution Statement
Design; Reliability; Shafts (machine element); Fatigue; Combined stress; Bending; Torsion	Unclassified - unlimited STAR category 37 (rev.)

19. Security Classif. (of this report)	20. Security Classif. (of this page)	21. No. of Pages	22. Price*
Unclassified	Unclassified	59	$3.75

* For sale by the National Technical Information Service, Springfield, Virginia 22151

CONTENTS

RELIABILITY APPROACH TO ROTATING-COMPONENT DESIGN

by Dimitri B. Kececioglu* and Vincent R. Lalli

Lewis Research Center

SUMMARY

The Lewis Research Center, in conjunction with the University of Arizona, has developed a design-by-reliability methodology for rotating mechanical components that statistically matches the selected material strength to the imposed stresses. Analytical and experimental methods have been developed to match materials and loads in this way. Design-by-reliability variables are handled as random functions. To illustrate this methodology, statistical methods for (1) determining strength distributions for steel experimentally, (2) determining a failure theory for stress variations in a rotating shaft subjected to reversed bending and steady torque, and (3) relating strength to stress by reliability are given in this report. The experimental test machines that provided data for the stress used with the design-by-reliability methodology are described.

A sample rotating component design problem is solved using both a deterministic design method and the proposed method. With the proposed method a smaller, lower weight shaft can result for a specified life and reliability than that with conventional methods. The new design-by-reliability methodology uses the distortion-energy theory with statistical fatigue diagrams for optimum shaft design. The conventional deterministic design methodology uses single-valued estimates, which results in unnecessarily conservative rotating component design. Other mechanical components, such as springs, bearings, gears, clutches, brakes, couplings, linkages, and cams, may also be designed using the design-by-reliability methodology.

INTRODUCTION

Present mechanical design techniques depend heavily on "modifying factors," such as, surface condition, size, temperature, stress concentration, and miscellaneous effects, to compensate for our limited knowledge of materials and loads. In the best

*Professor of Aerospace and Mechanical Engineering, the University of Arizona, Tucson, Arizona.

cases they are based on empirical data obtained over a long period of time, but in many others there are few data, and the selection is based on the designer's feelings at the time. A final factor that is often applied and that generally reflects all the uncertainties involved is probably influenced as much by the seriousness of the consequences should the part fail as by anything else. The resulting design is considerably larger and heavier than necessary to avoid failure.

Smaller and lighter designs are important in aerospace technology. Lighter designs are possible if the designs are based on the statistical matching of the available strength to the imposed stress. Lewis Research Center in conjunction with the University of Arizona in 1964 undertook the task of developing a mechanical design methodology of this type. The design methodology developed reduced the number of modifying factors by providing increased knowledge through laboratory testing methods. It deals with important design variables as statistical distributions rather than as single-value estimates. It also makes provisions to design for a specified life and reliability. To work out this methodology the following information is required:

(1) Statistical strength distributions for selected materials

(2) Statistical stress variations in a loading configuration

(3) Statistical methods for relating stress to strength.

This report presents the analytical, experimental, and application results attained in this research.

A typical rotating component design problem is given in appendix A to illustrate the deterministic, single-valued design technique. In appendix B the sample problem is worked out using the probabilistic design-by-reliability methodology which shows that substantial size and weight savings are accomplished. Very useful probabilistic experimental data for AISI 4340 steel are also presented. All data referenced in this report were taken using U. S. Customary units. To broaden the usefulness of the report, the U. S. Customary values were converted to International System (S. I.) values. The primary conversion factors are (1) 1 kilogram is 0.45 pound mass and (2) 1 kilonewton is 4.44 pounds force. The S. I. units are the primary reporting values, with the U. S. Customary values given as the second set throughout.

SYMBOLS

A, B, C	coefficient, staircase test
C_D	effect of size
C_L	effect of type of load
C_S	effect of surface finish

c	specimen radius, cm (in.)
D	specimen major diameter, cm (in.)
D_{max}	maximum specimen major diameter, cm (in.)
D_{cr}	critical specimen major diameter, cm (in.)
d	diameter
d_g	specimen groove diameter, cm (in.)
d_i	specimen stress increment, N/m^2 (psi)
E	Young's modulus, N/m^2 (psi)
G	gage factor
I	moment of inertia, cm^4 ($in.^4$)
i	staircase test method stress levels
J	polar moment of inertia, cm^4 ($in.^4$)
K_b	theoretical bending concentration factor
K_c	reliability factor
K_f	theoretical fatigue reduction concentration factor
K_{kw}	theoretical keyway concentration factor
K_s	theoretical torsional shear concentration factor
K_t	theoretical part geometry factor
K_v	theoretical constant value
$\mathscr{K}_{BGR}$	bending in groove coefficient
$\mathscr{K}_{BTH}$	bending to tool holder coefficient
$\mathscr{K}_{B/T}$	bending interaction into torque coefficient
$\mathscr{K}_{GRTH}$	groove to tool holder coefficient
$\mathscr{K}_L$	life cycles coefficient
$\mathscr{K}_T$	tool holder torque coefficient
$\mathscr{K}_{T/B}$	torque interaction into bending coefficient
$\mathscr{K}_V$	variation coefficient
$k_{a, b, c, d, e, f}$	modifying factors in eq. (3)
L_b	breaking tensile load, kN (lbf)

L_{ut}	ultimate tensile load, kN (lbf)
L_y	yield tensile load, kN (lbf)
M	bending moment on specimen, m-N (ft-lb)
N_a	number of active arms in strain bridge
N_c	Visicorder divisions
N_f	cycles to failure
N_v	Visicorder
N_1	number of specific cycles of life
n	sample size
n_i	number of successes at i^{th} level
n_s	number of specimens
$\mathscr{P}$	probability
pdf	probability density function
q	notch sensitivity factor
R_c	calibration resistance, ohm
R_g	gage resistance, ohm
$\mathscr{R}$	reliability
r	stress ratio, s_a/s_m
S_a	alternating probabilistic Goodman diagram material strength, N/m^2 (psi)
S_b	tensile breaking strength, N/m^2 (psi)
S_m	mean probabilistic Goodman diagram material strength, N/m^2 (psi)
S_n	corrected endurance limit, N/m^2 (psi)
S'_n	estimated endurance limit of the rotating beam specimen, N/m^2 (psi)
S_{ut}	tensile ultimate strength, N/m^2 (psi)
S_y	tensile yield strength, N/m^2 (psi)
s	stress
s_a	alternating material stress, N/m^2 (psi)
s_c	component strength standard deviation, N/m^2 (psi)
s_f	specific component strength, N/m^2 (psi)
s_m	mean material stress, N/m^2 (psi)

s_n	combined stress vector
s_o	lowest staircase level material stress, N/m^2 (psi)
T	torque, N-m (lb-ft)
x, y, z	normal random variables
z	standardized normal variable
α_3	skewness moment
α_4	kurtosis moment
Δ	tolerance, cm (in.)
ζ	difference statistic, N/m^2 (psi)
θ	angle, deg
μ	mean estimate
σ	standard deviation estimate
$\sigma_{x,a}$	alternating bending stress, N/m^2 (psi)
$\sigma_{x,c}$	compression bending stress, N/m^2 (psi)
$\sigma_{x,m}$	mean bending stress, N/m^2 (psi)
$\sigma_{x,n}$	notch bending stress, N/m^2 (psi)
$\sigma_{x,o}$	output bending stress, N/m^2 (psi)
$\sigma_{x,t}$	tension bending stress, N/m^2 (psi)
$\sigma_{y,a}$	alternating radial stress, N/m^2 (psi)
$\sigma_{y,m}$	mean radial stress, N/m^2 (psi)
$\tau_{xz,a}$	alternating shear stress, N/m^2 (psi)
$\tau_{xz,m}$	mean shear stress, N/m^2 (psi)
$\tau_{xz,n}$	notch shear stress, N/m^2 (psi)
$\tau_{xz,o}$	output shear stress, N/m^2 (psi)

Superscript:

$\bar{}$ mean of statistically distributed variables

BACKGROUND

The basic probabilistic methodology for designing mechanical components from a study of the intersection of their stress and strength distributions was discussed in

reference 1. Included in that paper was a discussion of Monte Carlo techniques for determining the stress and strength distributions, given the distributions of the factors affecting them.

Freudenthal (ref. 2) found in his study of structural unreliability that the safety factor was a random variable, which was the quotient of strength to stress, where both strength and stress were considered random variables. Freudenthal, Garrelts, and Shinozuka prepared a comprehensive report (ref. 3) along the same lines which discussed in more detail the mathematical techniques required, the appropriate statistical distributions involved, and problems that remained. Several example problems in structural reliability were worked out, and an extensive bibliography was given. These efforts concentrated on fatigue and structural reliability.

The Battelle Memorial Institute and its Mechanical Reliability Research Center presented studies (refs. 4 and 5) that described some of the fundamental problems in mechanical probabilistic design and suggested methods for their solution.

Mittenbergs (ref. 4) discussed the fundamental aspects of probabilistic design as applied to mechanical components. In that paper it was explained that the basic failure modes of mechanical components are (1) deformation, (2) fracture, and (3) structural instability. The combined effects of the various failure modes must be determined to assess the reliability of a mechanical component. The intersection of strength and stress distributions was discussed. Reference 5, a summary of 2 years of research, contains a thorough discussion of probabilistic design and attempts to quantify the relations of various factors on such phenomena as creep and fatigue. An extensive bibliography is included.

The Illinois Institute of Technology Research Institute conducted an extensive program (ref. 6) in probabilistic design methods. The program was concerned with three major areas: (1) The study of prime failure mechanisms in mechanical design (specific items included fatigue, wear, creep, and corrosion), (2) the application of failure mechanisms and design information for the reliability assessment of specific mechanical components (Parts included were gears, bearings, springs, and shafts.), and (3) the determination of mechanical system reliability in terms of individual component reliabilities.

Bratt, Reethof, and Weber (ref. 7) provided a computer approach to the solution of the time variant strength distribution case. Haugen (ref. 8) contributed to the understanding of probabilistic loads and their combinations. This work considers two aspects of the probabilistic design methodology: (1) the probability theory necessary to perform the design function and (2) probabilistic design examples drawn from various engineering disciplines.

Much still remained to be done. Important aspects of the design by reliability methodology that remained to be investigated were

(1) The development of the design by reliability methodology for specific cases
(2) The examination of methods to combine functions of random variables as applied to design by reliability
(3) The exploration of current and new methods for determining failure-governing stress and strength distributions
(4) The exploration of current and new methods for determining reliability once the failure-governing stress and strength distributions are known
(5) The development and fabrication of testing machines to provide data for the design by reliability methodology
(6) Carrying out a test program to obtain experimental materials data for use in the probabilistic, mechanical, design-by-reliability methodology.

This research included a literature search, a review of existing theory, design, development, and fabrication of test machines; experimental testing; and the development of computer programs to facilitate the reduction of the experimental data.

The research effort concentrated on the rotating shaft problem. This methodology demonstrates that other mechanical components, such as springs, bearings, gears, clutches, brakes, couplings, linkages, and cams can be designed by using reliability methods. Six reports (refs. 9 to 15) on this subject describe various aspects of the problem of designing rotating components that are subjected to combined-stress fatigue by the design-by-reliability methodology. Included are many aspects of estimating distributions, estimating stress and strength factors, computing reliabilities by various methods, and experimental test procedures. This report describes a probabilistic methodology for designing rotating mechanical components using reliability to relate stress to strength and the experimental data obtained to support this methodology.

ANALYSIS

Determine the Failure Governing Strength

In the engineering application of the disign-by-reliability methodology, one of the most difficult tasks is to determine the actual strength distribution of a specific material in a specific application. Two methods of determining this distribution are synthesis and direct experimentation. Much work remains to be done in these areas.

Synthesis. - Synthesis is concerned with finding a statistical function that accurately represents the material's strength. Considerable research has been expended by Kececioglu (ref. 11) and others to determine which distribution defines the experimental data best. The distributions studied are the normal, the lognormal, and Weibull.

A procedure to convert readily available tensile strength data, such as that given in table A-3 of reference 16 (p. 600) to statistical functions that accurately represent the material's endurance strength would be very useful. This table gives tensile yield strength S_y and tensile ultimate strength S_{ut}. In many cases where endurance strength distribution data for AISI steels are not available, use can be made of the common practice, based on the work of Lipson and Juvinall (ref. 17, p. 162), to obtain the estimate of the mean for endurance limit for steels as

$$\overline{S'_n} = 0.50\ S_{ut} \qquad \text{when } \bar{S}_{ut} \leq 1378\ \text{MN/m}^2\ (200\ \text{ksi}) \tag{1}$$

$$\overline{S'_n} = 689.4\ \text{MN/m}^2\ (100\ \text{ksi}) \qquad \text{when } \bar{S}_{ut} > 1378\ \text{MN/m}^2\ (200\ \text{ksi}) \tag{2}$$

The standard deviation for the normal distribution can be obtained by making use of a conclusion based on Kececioglu's and others' work (refs. 9 and 10). These investigators have found that a standard deviation of about 7 percent of the unmodified endurance limit can be used if little or no test data are available. The final expression[1] of S'_n becomes $(S'_n;\ 0.07\ S'_n)$.

Marin's work (ref. 17, p. 127) can be extended to obtain a machined part's distributional endurance limit S_n by considering each parameter in equation (3) as a random variable.

$$S_n = k_a k_b k_c k_d k_e k_f S'_n \tag{3}$$

The distribution of products of random variables can be calculated by various methods (refs. 18 and 19). Appendix B is an example of such a calculation. In this case (eq. (3)) k_a, k_b, and k_e have a value of unity because the experimental results include these factors. The reliability factor k_c is included by a different method, and S'_n is based on experimental data rather than on those data obtained from tables as explained previously. Appendix C gives the algebra of normal functions method of forming this product.

Another procedure for determining the distribution of the fatigue strength of materials is the Monte Carlo technique. References 9 and 20 to 23 disclose a correlation between the methods used in this report and these Monte Carlo techniques. Results obtained from the Monte Carlo computer calculations are within 5 percent of those obtained by the algebra of normal functions method when the coefficients of variation are small (ref. 9). Considering the experimental errors associated with strength of materials measurements, this normal functions method is a simpler and more acceptable procedure for estimating strength distributions under these conditions.

[1]Normal distribution notation (mean; standard deviation).

Direct experimentation. - In some cases it may not be possible to estimate the distribution parameters for the fatigue strength of a material. This almost always is due to a lack of statistically meaningful test data or engineering experience with a particular material. A laboratory test procedure by which fatigue strength for different materials could be obtained is desired.

The first requirement would be to design suitable test specimens. Specimens must be carefully prepared and inspected to insure that they reproduce as many of the essential features of the part application as possible (ref. 24). It is often necessary to scale the test specimens to retain the same stresses, stress concentration factors, stress ratios, and material conditions in a size suitable for testing. A meaningful quantity of these test specimens is required. A machine to test the specimens under conditions similar to the part application was also needed.

In this research two types of specimens were used. These are shown in figures 1 and 2 and are identified as specimen phases I and II. Groups of these specimens were tested to failure under fixed simulated environmental conditions. Table I shows the average stress levels, stress ratios and number of specimens tested. Figures 3 and 4 show the nine distributional stresses as functions of cycles (S-N) diagrams obtained from this environmental testing. Carefully prepared specimens were subjected to fixed levels of alternating and shear stresses to keep the average stress ratio (alternating/mean) $\bar{r}$ at fixed values.

Endurance tests were conducted using the "staircase" method (ref. 26). The results are given in table II. This information was used to obtain the distributional Goodman diagrams of figure 5. This was accomplished by projecting the endurance strength test data to the appropriate stress ratio planes as shown in figure 5(a). Table II shows the alternating endurance strength distribution parameters at 25° C from the analysis of the test data and the components of the distribution parameters along the various stress ratio planes.

If a probabilistic Goodman diagram for rotational lives shorter than 2.5×10^6 cycles is desired, diagrams similar to that in figure 5 can be generated by the method shown graphically in figure 6. The cycles to failure distributions given in figures 3 and 4 for a particular stress ratio and cycles of life are summed. The cumulative histogram is formed to show the percentage of specimens failing in each stress cell for a fixed cycle life value. From this histogram, the material's combined strength distribution can be found (ref. 25). The resulting statistical distribution is the material's strength for a fixed number of cycles of life and stress ratio. However, the components of strength distribution along the fixed stress ratio plane are needed for specific shaft design problems. These strength distribution components can be obtained as follows:

(1) Obtain values for S_a, σ_{S_a}, r, and N_1 from figure 6.

(2) It is known that

$$S_f = \left(S_a^2 + S_m^2\right)^{1/2} \tag{4}$$

and

$$\bar{r} = \frac{\bar{S}_a}{\bar{S}_m} \tag{5}$$

(3) Substitute equation (5) into equation (4) and obtain

$$\bar{S}_f = \left[\bar{S}_a^2 + \left(\frac{\bar{S}_a}{\bar{r}}\right)^2\right]^{1/2} \tag{6}$$

(4) Simplify equation (6) and assume that S_f and S_a are normally distributed and that r is a fixed plane.[2] This yields

$$\bar{S}_f = \bar{S}_a\left(1 + \frac{1}{\bar{r}^2}\right)^{1/2} \tag{7}$$

and

$$\sigma_{S_f} = \sigma_{S_a}\left(1 + \frac{1}{\bar{r}^2}\right)^{1/2} \tag{8}$$

Substituting test values into equations (7) and (8) yields the mean and standard deviation components of the strength distribution along $\bar{r}$ for the probabilistic Goodman diagram. It seems that, to establish an acceptable Goodman fatigue strength surface, at least four such distributions ($r = \infty$, 3.5, 0.83, and 0.44 at a specified life cycle) are required. This, coupled with the static ultimate tensile strength distribution at $\bar{r} = 0$, gives five sections on the contour to define the probabilistic Goodman strength surface.

[2]Consideration of r as a random variable complicates matters considerably. The six standard deviations variation should not be greater than ±0.017 rad (±1°) for most cases; therefore, $\bar{r}$ was fixed as a plane.

Determine the Failure Governing Stress

The first problem in determining the failure governing stress is to identify the failure governing theory which applies best to the part in service considering its material, loads, dimensions, stress concentrations, and the like. Rotating shafts have been analyzed using the distortion-energy or von Mises-Hencky failure criterion (refs. 9 and 27). This distortion-energy criterion is applicable to ductile steels (ref. 9, pp. 152-154) and is theoretically valid for the elastic region only. It is recognized that the steel used in this research does not strictly fit the ductile requirement. Although the fracture pattern in fatigue of these grooved specimens is ductile; in direct tension the fracture pattern is brittle. The elastic region constraint is not strictly met either, as the specimens are tested to fracture. The methodology exhibited in this report assumes that the distortion-energy theory describes the material stresses that cause failure. Test results indicate that other failure theories, combinations of theories, or newly developed theories may also accurately reflect the laboratory results (refs. 9, 27, and 28) and they should also be studied.

Figure 7(a) shows the rotating shaft volume element stresses for the general case. For the specific case of a rotating shaft subjected to bending and torque stresses only, the xz element at the surface simplifies (see fig. 7(b)). Using the stress components as defined in figure 7(b) and the von Mises-Hencky failure criterion (ref. 16, p. 154), the failure governing alternating stress s_a is given by

$$s_a = \sigma_{x,a} \tag{9}$$

and the failure governing mean stress s_m by

$$s_m = \sqrt{3}\,\tau_{xz,m} \tag{10}$$

For this stress model, the following design-by-reliability equations can be derived:

$$s_f = s_a \left(1 + \frac{1}{\bar{r}^2}\right)^{1/2} \tag{11}$$

and

$$\sigma_{s_f} = \sigma_{s_a}\left(1 + \frac{1}{\bar{r}^2}\right)^{1/2} \tag{12}$$

where

$$\bar{s}_a = \frac{\bar{M}}{\bar{I}/c} = 10.2\,\frac{\bar{M}}{\bar{d}^3} \tag{13}$$

$$\sigma_{s_a} = 129.7\,\frac{1}{\bar{d}^3} \tag{14}$$

and

$$\bar{r} = \frac{\bar{s}_a}{\bar{s}_m} \tag{15}$$

Appendix B gives a detailed example for the use of these equations.

Bridge the Gap by Reliability

Using reliability to relate material strength to application stresses requires the identification of all failure modes and the sections where these failures may occur. For each such section and failure mode the failure governing strength and stress distributions should be determined next, and finally the reliability should be calculated as follows:

A no failure probability exists for the critical failure mode and section when a given strength S is not exceeded by a given stress s (ref. 1, p. 555). From figure 8, the probability that a stress of value s_1 exists in the interval $s_1 - ds/2$ to $s_1 + ds/2$ is equal to the area of the element ds (A_1 as shown in fig. 8) or

$$\mathscr{P}\left(s_1 - \frac{ds}{2} \le s \le s_1 + \frac{ds}{2}\right) = f(s_1)ds = A_1 \tag{16}$$

The probability that S exceeds s_1 is equal to the shaded area A_2 in figure 8, or

$$\mathscr{P}(S > s_1) = \int_{s_1}^{\infty} f(S)dS = A_2 \tag{17}$$

The probability of no failure is the product of these two probabilities or

$$d\mathscr{R} = f(s_1)ds\left[\int_{s_1}^{\infty} f(S)dS\right] \tag{18}$$

The section's reliability would then be all probabilities of all strengths being greater than all possible values of stress or

$$\mathscr{R} = \int d\mathscr{R} = \int_{-\infty}^{\infty} f(s)\left[\int_{s}^{\infty} f(S)dS\right]ds \tag{19}$$

The section reliability can also be written as (ref. 1, p. 556)

$$\mathscr{R} = \int_{-\infty}^{\infty} f(S)\left[\int_{-\infty}^{S} f(s)ds\right]dS \tag{20}$$

Equations (19) or (20) can now be used to calculate the critical section's reliability for any component whose f(s) and f(S) are known. These equations carry limits of integration applicable to distributions defined over the interval from $-\infty$ to $+\infty$. For functions defined in different intervals these limits should be replaced by the lowest and highest values that can be used. For methods of evaluating equations (19) and (20) see references 1 and 25 when neither f(s) and f(S) is normal or lognormal.

If both f(s) and f(S) are normal, the probability density functions may be expressed as

$$f(s) = \frac{1}{\sigma_s\sqrt{2\pi}} e^{-1/2[(s-\bar{s})/\sigma_s]^2} \tag{21}$$

and

$$f(S) = \frac{1}{\sigma_S\sqrt{2\pi}} e^{-1/2[(S-\bar{S})/\sigma_S]^2} \tag{22}$$

The critical section reliability is given by the probability that strength is in excess of stress or that $S - s > 0$. Using the designation $\zeta = S - s$, the critical section reliability is given by all of the probabilities that $\zeta > 0$. Let $f(\zeta)$ be defined as the difference distribution of f(S) and f(s). As f(S) and f(s) are normally distributed, then

$f(\zeta)$ is also normally distributed and is expressed by (ref. 1, p. 556)

$$f(\zeta) = \frac{1}{\sigma_\zeta \sqrt{2\pi}} e^{-1/2\left[(\zeta - \bar{\zeta})/\sigma_\zeta\right]^2} \tag{23}$$

where

$$\bar{\zeta} = \bar{S} - \bar{s} \tag{24}$$

and

$$\sigma_\zeta = \left(\sigma_S^2 + \sigma_s^2\right)^{1/2} \tag{25}$$

The critical section reliability would then be given by all probabilities of ζ being a positive value, hence,

$$\mathscr{R} = \frac{1}{\sigma_\zeta \sqrt{2\pi}} \int_0^\infty e^{1/2\left[(\zeta - \bar{\zeta})/\sigma_\zeta\right]^2} d\zeta \tag{26}$$

The relation between ζ and the standardized normal variate z can be used to evaluate equation (26), which is

$$z = \frac{\zeta - \bar{\zeta}}{\sigma_\zeta} \tag{27}$$

The limit of the integrand for $\zeta = 0$ is

$$z = \frac{0 - \bar{\zeta}}{\sigma_\zeta} = -\frac{\bar{\zeta}}{\sigma_\zeta} \tag{28}$$

and for $\zeta = \infty$ is

$$z = \frac{\infty - \bar{\zeta}}{\sigma_\zeta} = \infty \tag{29}$$

also

$$d\zeta = \sigma_\zeta \, dz \tag{30}$$

If these conditions are substituted into equation (26), the following result is obtained:

$$\mathscr{R} = \int_{-(\bar{\zeta}/\sigma_\zeta)}^{\infty} \frac{1}{\sqrt{2\pi}} e^{-1/2(z^2)} dz \tag{31}$$

Consequently, the critical section reliability of a component is given by the area under the standardized normal probability density function from the value of $z = -(\bar{\zeta}/\sigma_\zeta)$ to $z = \infty$. The value of this area may be obtained from the table of areas under the standardized normal density function.

APPARATUS AND PROCEDURE

Combining reversed bending with steady torque for fatigue testing of metal specimens was previously tried by Mabie and Gjesdahl (ref. 29). Their paper explained a test machine using the four-square and rotating-beam principles. The four-square principle couples torque to a specimen through a connecting shaft, two end gear boxes, and a second shaft for torque loading. The rotating beam principle applies reverse bending through bearings and a static fixed force. These methods of applying combined stresses to metal test specimens without the need to dissipate energy proved satisfactory. However, this first machine was not able to hold torque or bending stresses constant, and developed excessive noise and vibration during operation.

Probabilistic design by reliability applied to space-power system shafts required that a test machine capable of providing constant torque and bending stresses for metal specimens be developed (ref. 30). Using the proven principles of the Mabie-Gjesdahl machine, the University of Arizona designed and built such a machine. The machine was carefully reviewed, modified where appropriate, and approved by Lewis.

Research Machine

The fatigue machine consists of a two-section, rotating shaft in the front with a test specimen locked in the center (fig. 9). The front shaft has a flexible coupling at each

end to allow for relatively free deflection when the specimen is loaded in bending. A direct 200-watt (7.5-hp), 1800-rpm motor powers the front shaft. The bending load is applied to the specimen by means of two yokes, one on each of two bearings located symmetrically about the specimen on two commercial tool holders. Below the shaft the yokes are connected by a horizontal link, which concentrates the load at a single vertical link in the center. The vertical link is then connected to either a long or a short loading lever arm. These loading arms make possible the application of a range of bending stresses in the specimen groove by means of pan weights applied at the end of the loading arm. The steady torque is applied by means of a commercial Infinit-Indexer which is located on the back shaft of the machine which rotates at about 1000 rpm. Table III summarizes the operational specifications of these research machines. The machine is capable of producing, holding, and transmitting to the rotating specimen steady torques of up to 605 newton-meters (5400 lb-in.) and reversed bending moments of up to 386 meter-newtons (3450 in.-lb). Specimens with diameters up to 2.5 centimeters (1 in.) can be tested in this machine by changing the collets in the specimen holder. This machine has the following advantages:

(1) A constant bending moment is maintained by directly applied static loads.

(2) Constant torque is maintained through the use of an Infinit-Indexer.

(3) Monitoring of specimen strain is reasonably direct.

(4) Backlash in the four-square loop is eliminated.

Typical space-power turbine shaft designs were analyzed to make the research data directly applicable to aerospace problems. Figures 1 and 2 show the grooved test specimen details (ref. 31). Bar stock pieces about 15 centimeters (6 in.) long were carefully machined to the dimensions and finish specified in figures 1 and 2. The reverse bending moment M, torque T, bending stress $\sigma_{x,a}$, and shear stress $\tau_{xz,m}$ are identified in figure 1.

Research Procedure

Each specimen is installed in the test machine, and the instrumentation is checked for zero adjustment and calibration. The appropriate bending moment is applied to the specimen by putting weights on the load pan. The torque is applied to the specimen by rotating the outer shell of the Infinit-Indexer with a suitable wrench. The timing clock is set to zero and the machine is started. When the specimen fractures, a microswitch stops the clock and the machine. Figures 1(b) and 10 show the specimen configuration and fracture pattern after testing, respectively.

Strain gages are used on the tool holder to monitor the bending and torque loads. These gages are located on the tool holder rather than on the specimen groove. The reasons for this are that (1) it is difficult to mount strain gages in the limited space of

a specimen groove and (2) because the specimens are fractured, the gages could also be damaged during failure resulting in prohibitive expenses. The positioning and electrical circuitry for the strain-gage bridges are given in figure 11. The slip-ring assembly is located next to the strain gages. The slip-rings are counterbalanced with an aluminum collar of equal weight and nearly equal dimensions located on the other tool holder (see fig. 9). The amplifiers, galvanometers, and recorder are matched units. This equipment is used to amplify and record the output from the bending and torque gages.

Measurement of the nominal bending and shear stresses in the specimen groove are required. Because the strain gages cannot be located in the specimen groove, the shear and bending stresses in the specimen groove must be determined from the tool holder strain gages. To convert tool holder strain data to specimen groove stresses, the following calibration coefficients were required:

(1) Actual groove bending stress versus apparent groove bending stress

(2) Apparent groove bending stress versus apparent tool holder bending stress

(3) Torque interaction into bending

(4) Actual groove shear stress versus tool holder shear stress

(5) Bending interaction into torque.

Each machine was carefully calibrated (ref. 12). The relation between the calibration variables, in each case, proved to be linear; hence, a slope could be associated with each calibration variable. Because for all cases the functional relation began at the origin, the slope alone of each curve completely defined the function. These slopes have been given calibration coefficient designations and are listed in table IV. The mode of use of the calibration results is described in detail in figure 12. Steps 1 and 2 require the selection of a stress ratio and a bending stress level. The nominal shear stress in the specimen groove to give this ratio is found in step 3. Next, in step 4 the nominal bending stress in the groove is converted to output stress in the groove using $\mathscr{K}_{BGR}$ and $\mathscr{K}_{GRTH}$. On the torque side, step 5 gives the equation for converting the nominal shear stress in the groove to shear stress in the tool holder. Also, in step 5 the shear stress in the tool holder is converted to output stress. Steps 6 and 7 are the corrections for interaction between torque and bending. Steps 8 and 9 convert the corrected output stress to Visicorder divisions, completing the procedure. Each machine has the following calibration equation: For bending B

$$N_{v,B} = \frac{N_c N_a GR_c}{ER_g} \left(\mathscr{K}_{BGR} \mathscr{K}_{GRTH} \bar{\sigma}_{nom,GR} + \mathscr{K}_{T/B} \bar{\tau}_{out,TH} \right) \tag{32}$$

and for torque T

$$N_{v,\,T} = \frac{N_c N_a G R_c}{E R_g}\left(\frac{\mathscr{K}_{BTH}}{\mathscr{K}_T}\,\bar{\tau}_{out,\,TH} + \mathscr{K}_{B/T}\bar{\sigma}_{out,\,TH}\right) \tag{33}$$

All strain-gage parameters are those of the bending and torque bridges.

For data reduction a stress ratio and a bending stress level in the groove are selected, as is shown in blocks 1 and 2 of figure 12. From these two parameters the nominal shear stress in the groove is determined in block 3. This step uses the distortion-energy failure criterion. Next, the nominal bending stress in the groove is converted to tool holder stress in block 4. In block 5 the theoretical conversion from the groove to tool holder torque and from nominal to output tool holder stress is made for shear. In blocks 6 and 7 each tool holder output is corrected for interaction effects. In blocks 8 and 9 the output tool holder stresses are converted to recorder divisions. Thus, the number of recorder divisions necessary to give the required stress ratio and bending stress level are determined.

Next, a sample is run while maintaining the necessary divisions of bending and torque as closely as possible. A record of the bending and torsion gage signals is taken for every specimen. When the running of the sample lot is complete, the data reduction procedure is reversed for each specimen to determine the nominal bending and shear stresses and the stress ratio actually achieved.

EXPERIMENTAL RESULTS

To reach the primary objectives of this research, it was necessary to obtain distributional S-N, endurance, and static tensile strength data. The research consisted of running test specimens under selected and controlled conditions for

$$\bar{r}_s = \frac{\bar{S}_a}{\bar{S}_m} = \frac{\bar{\sigma}_{x,\,a}}{\sqrt{3}\,\bar{\tau}_{xz,\,m}} = 0,\ 0.44,\ 0.83,\ 3.50,\ \infty$$

and

$$s_a = \sigma_{x,\,a}$$

ranging between 172.4 and 1034.1 newtons per square meter (25 and 150 ksi).

The number of specimens tested for each stress level of an S-N diagram was either 12 or 18. It was determined that three to six stress levels should be studied to ascertain the distributional S-N diagram for a particular stress ratio.

Tables I and II, V to VIII, and figures 3 and 4 present the types of data obtained from the research machines and the reduced results. Table I gives stress levels, ratios, and the cycles-to-failure data (life) for research phases I and II. Table II gives the endurance strength distribution results. Table V shows, as an example, how the endurance strength data for mean stress ratio of 0.44 are reduced to obtain their distribution parameters using the sample data given in figure 13. Table VI gives the grooved and ungrooved static tensile strength data as the strength data for $r = 0$. Tables VII and VIII summarize the parameters for the normal and the lognormal distributions fit to the cycles to failure (life) data. Figures 3 and 4 give the distributional S-N diagram presentation of the cycles to failure (life) results given in tables II, VII, and VIII in lognormal distribution form. An analysis of the cycles to failure data shows that the distributions are log-normally distributed; therefore, they plot as normal distributions on log-log scales (ref. 13). Figure 5 gives the probabilistic Goodman diagram for the phase I and II data given in table II in normal distribution form.

Figure 13 is a sample of the data for endurance strength testing. The endurance tests were conducted using the "staircase" method. In the staircase method the bending stress is changed in increments of about 20.7 meganewtons per square meter (3.0 ksi), while maintaining a constant stress ratio. If there is no failure during about a 2.5-million-cycle test, then one increment is added to the bending stress level of the next specimen and the test repeated. If a failure occurs, one increment is subtracted for the next specimen. The endurance strengths are best represented by normal distributions (ref. 10).

EXPERIMENTAL VERSUS EMPIRICAL S-N DIAGRAM

If the desired experimental S-N diagram is not available, the designer is forced to develop his own based on empirical considerations and long-established rules of thumb. To find out how good these rules-of-thumb are, the mean S-N diagrams determined experimentally in phase I were superimposed on the conventional thumb-rule developed S-N diagram in figure 14. The empirical S-N diagrams were constructed according to a procedure recommended by Juvinall (ref. 32, p. 211), knowing the ultimate strength of a given steel, as follows:

For the AISI 4340 steel used in this research, the ultimate strength S_{ut} was 1227.1 meganewtons per square meter (178 ksi) for unnotched specimens. The endurance strength at 10^6 cycles of life is given by (ref. 32, pp. 236-256)

$$S_{n_{10^6}} = \frac{S'_n C_L C_D C_S}{K_f} \tag{34}$$

where

$$S'_n = 0.5\, S_{ut} = 613.6 \text{ N/m}^2 \text{ (89 ksi)} \tag{35}$$

and where the effect of load type C_L equals 1.0 for bending, the effect of size C_D equals 0.9 for diameters between 1 and 5.08 centimeters (0.4 and 1 in.), the effect of surface finish C_S equals 0.88 for the fine ground finish, and the fatigue stress concentration factor K_f is

$$K_f = 1 + q(K_t - 1)C_S$$

where q is the notch sensitivity and K_t is the theoretical stress concentration factor obtained from Peterson's data (ref. 34, p. 49). Hence, for $q = 0.95$ and $K_t = 1.42$

$$K_f = 1 + 0.95(1.42)(0.88) = 1.351$$

Other factors, such as temperature effects, residual stresses, and surface defects, are considered to have no effect. Therefore, from equation (34)

$$S_{n_{10^6}} = \frac{(613.6)(1.0)(0.9)(0.88)}{1.351} = 360 \text{ MN/m}^2 \text{ (or } 52.2 \text{ ksi)}$$

The fatigue strength at 10^3 cycles is given by (ref. 32, pp. 260-263)

$$S_{n_{10^3}} = 0.9\, \frac{S_{ut}}{K'_f} \tag{36}$$

where

$$K'_f = 1 + (K_f - 1)Y \qquad Y = 0.64$$

and

$$S_{ut} = 1227.1 \text{ MN/m}^2 \text{ (or } 178 \text{ ksi)}$$

and where Y is the factor determined by Juvinall. Hence,

$$S_{n_{10^3}} = \frac{(0.9)(1227.1)}{1 + (0.351)(0.64)} = 901.7 \text{ MN/m}^2 \text{ (or } 130.8 \text{ ksi)}$$

In determining the empirical value of the strength at 10^3 cycle life, the unnotched ultimate strength has been used rather than the notched. To obtain the empirical rule-of-thumb based S-N diagram, a straight line is drawn on log-log paper between 901.7 meganewtons per square meter (130.8 ksi) at 10^3 cycles and 360 meganewtons per square meter (52.2 ksi) at 10^6 cycles. This is the empirical line in figure 14, and it represents the mean rule-of-thumb cycles-to-failure estimate. The remaining lines shown in figure 14 are the best-fit mean cycles-to-failure lines for the four stress ratios researched in phase I.

A comparison of Juvinall's method for constructing an empirical S-N diagram with the experimentally determined mean line for a stress ratio of infinity shows the strength at 10^3 cycles is underestimated using Juvinall's method and the mean value of the tensile strength of the unnotched specimens. At 10^3 cycles the empirical estimate of the mean fatigue strength yielded a value of about 901.7 meganewtons per square meter (130.8 ksi) compared with 1172 meganewtons per square meter (170 ksi) for a stress ratio of infinity, or 75 percent of actual. At the other end of the diagram the empirical estimate of the endurance strength yielded a value of 360 meganewtons per square meter, which is below the experimentally determined mean value of 395 meganewtons per square meter for a stress ratio of infinity, or 9 percent lower than actual, thus making the empirical estimate conservative. Furthermore, the empirical life of 10^6 cycles is high when compared with the experimental value of 700 000 cycles for a stress ratio of infinity. Specifically, it is 43 percent higher; consequently, the empirically established endurance life is not conservative. Since Juvinal does not take into account complex loading involving alternating bending and constant mean torsion, the empirical S-N diagram will only be applicable for the stress ratio of infinity.

DESIGNED EXAMPLE

A typical rotating component part design problem is given in appendix A. The part is the inner shaft of an alternator rotor, shown in figure 15(b). It is designed first using a deterministic, single-valued design methodology and modifying factors to reduce the material's endurance limit to the case of the problem. A Goodman boundary limit is constructed using the modified endurance limit with existing tensile strength data. The distortion-energy stress components suitable for this model are theoretically selected. Finally, graphical construction methods are used to determine the permissible alternating and mean stress for this material. The desired shaft diameter is calculated using equation (46) of appendix A. The results of this design effort are summarized in

table IX, where values are given for the important design parameters. The shaft diameter following this design procedure came out to be 1.39 centimeters (35/64 in.).

The same shaft is redesigned using the methodology in appendix B. This method does not require modifying factors for surface finish, size, or stress concentration as the laboratory test program generated data for endurance strengths under combined conditions of reversed bending and steady torque for machined and ground test specimens of about the proper size and with very similar stress concentration. The distributional Goodman diagram of figure 5(a) is used to determine the failure governing strength distribution for this material. The desired shaft diameter is calculated using the difference statistics of two normal distributions resulting in equation (63) in appendix B. The results of this probabilistic design effort are also summarized in table IX. The shaft diameter following the probabilistic design procedure came out to be 1.04 centimeters (27/64 in.). This is a 40-percent decrease in the weight of material required to fabricate this part. Furthermore, the design is estimated to have a shaft life of 2.5×10^6 cycles and a minimum reliability of 0.999; that is, it is expected that no more than 1 in 1000 such shafts will fail while performing their designed-for mission.

Using reliability to relate material strength to application stresses requires careful engineering judgment to assess all failure modes. A given design requires that the most likely section to fail and its failure mode be selected and analysis performed at that section. In the probabilistic design-by-reliability approach none of the original design requirements were reduced. These requirements were met by selecting the most probable failure mode and matching it with the material, geometry, and appropriate fatigue strength.

The best designed product is only as good as the people and materials finally used to make it. The task of determining that people with the required skills and materials of the proper specified quality are used to build the product must be included in this design methodology by other means. This task requires participation of many disciplines including rigorous quality assurance engineering (ref. 24). There are many important design problems that can be solved using the probabilistic design-by-reliability concepts developed in this research. Other problems and their solutions using this methodology can be found in the literature (refs. 1, 8, 9, 13, 25, and 35 to 37).

DISCUSSION OF RESULTS

The research results are summarized in tables I, II, V to VIII and figures 3 and 4 (distributional S-N diagrams), figure 14 (comparison of the experimental S-N diagram with the theoretical), figure 5 and table II (distributional Goodman diagrams), and table IX (comparison of results of conventional design with probabilistic design-by-reliability results).

The combined-stress fatigue research machines are capable of applying and maintaining the desired alternating bending moment and steady torque, based on the low achieved ratio of $\sigma_r/\bar{r}$. These machines enable the application of about 390 meter-newtons (3450 in. -lb) of bending moment and about 600 newton-meters (5400 lb-in.) of torque to the test specimen.

Probabilistic analysis of the S-N data reveals that the cycles-to-failure distributions for various stress ratios are best represented by the lognormal distribution; whereas the endurance strength distributions are best represented by the normal distribution.

For phase I results and $\bar{r} = \infty$ the mean cycle life increases substantially as the nominal alternating bending stress decreases from about 1170 to 480 meganewtons per square meter (170 to 70 ksi). Specifically, the mean of the cycles to failure at 965 MN/m^2 (140 ksi) is about 2900 cycles, and at 480 MN/m^2 (70 ksi) the mean of the cycles to failure is about 187 800 cycles, or a 53 percent increase. The standard deviation of the cycles to failure at 965 MN/m^2 (140 ksi) is $\sigma_{\log_e N} = 0.172$; at 480 MN/m^2 (70 ksi) it is $\sigma_{\log_e N} = 0.192$, or an 11 percent increase on the basis of the logs. It must be pointed out that a comparison of the standard deviation on the basis of the straight cycles cannot be made because the cycles-to-failure distribution is lognormal and the antilog of $\sigma_{\log_e N}$ does not provide any useful information. The standard deviation does increase, however, as the alternating stress level decreases although not much for $r = \infty$.

Figure 3(b), the distributional S-N diagram for $r = 3.5$, shows a substantial increase in the mean cycle-life as the nominal alternating bending stress decreases from about 1170 to 480 MN/m^2 (170 to 70 ksi). Specifically, the mean of the cycles to failure at 965 MN/m^2 (140 ksi) is about 2100 cycles and at 480 MN/m^2 (70 ksi) is about 98 000 cycles, or a 50 percent increase on the basis of the logs. The standard deviation of the cycles to failure at 965 MN/m^2 (140 ksi) is $\sigma_{\log_e N} = 0.180$; at 480 MN/m^2 (70 ksi) it is $\sigma_{\log_e N} = 0.286$, or a 59 percent increase on the basis of the logs. In this case the standard deviation increases substantially as the alternating stress level decreases for $r = 3.5$ as compared with the situation for $r = \infty$.

Figure 3(c), the distributional S-N diagram for $r = 0.83$, likewise shows a substantial increase in the mean cycle-life as the nominal alternating bending stress decreases from about 830 MN/m^2 (120 ksi) to about 480 MN/m^2 (70 ksi). Specifically, the mean of the cycles to failure at 830 MN/m^2 (120 ksi) is about 4300 cycles and at 480 MN/m^2 (70 ksi) is about 88 200 cycles, or a 36 percent increase on the basis of the logs. The standard deviation of the cycles to failure at 830 MN/m^2 (120 ksi) is $\sigma_{\log_e N} = 0.197$; at 480 MN/m^2 (70 ksi) it is $\sigma_{\log_e N} = 0.197$, an increase of only 0.4 percent. This increase is even less than that for $r = \infty$; nonetheless, it is an increase in the standard deviation as the alternating stress level decreases.

Figure 3(d), the distributional S-N diagram for $r = 0.44$, shows a smaller increase in the mean cycle life as the nominal alternating bending stress decreases than for the other stress ratios, but the range of the alternating bending stress is also smaller, namely, from about 550 MN/m^2 (80 ksi) to about 415 MN/m^2 (60 ksi). Specifically, the mean of the cycles to failure at 550 MN/m^2 (80 ksi) is about 19 100 cycles; at 415 MN/m^2 (60 ksi) it is about 130 500 cycles, or an increase of 20 percent. The standard deviation of the cycles to failure at 550 MN/m^2 (80 ksi) is $\sigma_{\log_e N} = 0.245$; at 415 MN/m^2 (60 ksi) it is $\sigma_{\log_e N} = 0.329$, or an increase of 34 percent. Thus, the standard deviation likewise increases as the alternating stress level decreases.

Conclusions similar to these may be drawn from a study of figure 4, for phase II results.

A study of figure 3 shows that the following maximum nominal alternating bending stress levels are permissible for phase I results: For $r = \infty$, $S_{a, max} = 1700$ MN/m^2 (170 ksi), for $r = 3.5$, $S_{a, max} = 1170$ MN/m^2 (170 ksi), for $r = 0.83$, $S_{a, max} = 860$ MN/m^2 (125 ksi), and for $r = 0.44$, $S_{a, max} = 535$ MN/m^2 (78 ksi) to avoid imposing bending and shear stresses in the vicinity of the yield strength of the material.

A study of figure 4 shows that the following maximum nominal alternating bending stress levels are permissible for phase II results: For $r = \infty$, $S_{a, max} = 895$ MN/m^2 (130 ksi); for $r = 1.06$, $S_{a, max} = 830$ MN/m^2 (120 ksi); for $r = 0.40$, $S_{a, max} = 375$ MN/m^2 (55 ksi); for $r = 0.25$, $S_{a, max} = 310$ MN/m^2 (45 ksi); and for $r = 0.15$, $S_{a, max} = 225$ MN/m^2 (37 ksi).

A comparison of figure 3 and a study of table III, all for phase I results, indicate that, for the same alternating stress level, as the stress ratio decreases from ∞ to 0.44 the mean life also decreases. In particular, at a nominal alternating stress level of 480 MN/m^2 (70 ksi) the following mean lives are exhibited: For $r = \infty$ about 187 800 cycles, for $r = 3.5$ about 98 100 cycles, for $r = 0.83$ about 88 200 cycles, and for $r = 0.44$ about 46 600 cycles. It is apparent that there is a significant reduction in the mean life as the shear stress, which is superimposed onto the bending stress, is increased, that is, as the stress ratio is decreased. From $r = \infty$ to 3.5 the mean life (in cycles) is reduced by 48 percent; from $r = 3.5$ to 0.83 the mean life is reduced by 10 percent; and from $r = 0.83$ to 0.44 the mean life is reduced by another 47 percent.

A comparison of figure 4 and a study of table II for phase II indicate that similar conclusions may be drawn for phase II results.

A further comparison of figure 3 and a study of table II indicate that, as the stress ratio decreases from ∞ to 0.44, the standard deviation of the cycles to failure increases in general. In particular at a nominal alternating stress level of 480 MN/m^2 (70 ksi) the following standard deviations are exhibited: For $r = \infty$, $\sigma_{\log N} = 0.192$; for $r = 3.5$, $\sigma_{\log N} = 0.286$; for $r = 0.83$, $\sigma_{\log N} = 0.197$; and for $r = 0.44$, $\sigma_{\log N} = 0.274$. These data show that standard deviation increases in terms of $\log_{10}$ cycles to

failure, as the stress ratio decreases. A similar trend may also be observed for other alternating stress levels.

A comparison of figures 3(a) and 4(a) shows that at an alternating bending stress level of 480 MN/m^2 (70 ksi) and $r = \infty$, the mean cycles to failure decreases from about 187 800 cycles for phase I to about 12 800 cycles for phase II results, or a 93 percent decrease. This sharp reduction in the mean life results when the groove geometry is so altered that its theoretical stress concentration factor increases from 1.42 to 2.34. Consequently, great care must be exercised not to introduce such high stress concentrations.

A comparison of figures 3 and 4 indicates that, as the theoretical stress concentration factor is increased from 1.42 to 2.34, the standard deviation of the cycles-to-failure decreases because of the greater concentration of stress in a smaller volume of groove material and the higher actual stresses in the groove.

A study of figure 14 indicates that for $r = \infty$ Juvinall's method for constructing an empirical S-N diagram underestimates the fatigue strength at 10^3 cycles of life by about 25 percent because the experimental alternating bending strength at 10^3 cycles is 1170 MN/m^2 (170 ksi) instead of the 901.7 MN/m^2 (130.8 ksi) predicted by Juvinall's empirical method. It appears that either one or both factors that determine the empirical fatigue strength at 10^3 cycles (eq. (36)) ought to be modified. Specifically, if it is assumed that the fatigue stress concentration factor K_f' is the best available to date, a correction for the 0.9 factor would be in order such that the new factor for this material and geometry would be 1170/1176 (170/178) = 0.955.

Figure 14 indicates that the mean endurance strength at 10^6 cycles of life is also underestimated by Juvinall's empirical method. Specifically, the experimental value is 395 MN/m^2 (57.3 ksi) as compared with 360 MN/m^2 (52.2 ksi) for the empirical estimate. A study of equations (34) and (35) indicates that the potential contributors to this difference might be primarily the factor of 0.5 in equation (35) and the factor C_D or size effect in equation (34). It may be assumed that, because of lack of good recent data on C_D, the correction may best be made on the factor 0.5, which could be modified to 395/360 (57 300/52 200) = 0.549. Therefore, equation (35) would now be

$$S_n' = 0.549\, S_{ut} \tag{37}$$

It is of interest to compare the cycles of life at the knee of the empirical S-N diagram with that of the experimental S-N diagram for $r = \infty$. It may be seen that the experimental endurance life is 700 000 cycles as compared with 10^6 cycles for the theoretical of Juvinall, or 30 percent lower. Furthermore, even greater reductions in the endurance life result from the superimposing of a constant torsional shear stress onto the alternating bending stress; namely, the life at the knee is 300 000 cycles for $r = 3.5$, 270 000 cycles for $r = 0.83$, and 550 000 cycles for $r = 0.44$.

A study of table II(a) indicates that, as the stress ratio decreases from ∞ to 0.45, the endurance strength under combined bending-torsion decreases from a nominal alternating bending stress of 395 MN/m^2 (57.3 ksi) to 341.9 MN/m^2 (49.6 ksi), or a 13 percent decrease, which points out the significant effect on the mean endurance strength of the superimposition of increasing torsional shear stress onto the alternating bending stress at 2.5×10^6 cycles of life.

A study of table II(b) indicates that, as the stress ratio decreases from ∞ to 0.15, the endurance strength under combined bending-torsion decreases from a nominal alternating bending stress of 232.3 MN/m^2 (33.7 ksi) to 157.9 MN/m^2 (22.9 ksi), or a 34 percent decrease. This decrease, again, points out the significant effect on the mean endurance strength of the superimposition of increasing constant torsional shear stress onto the alternating bending stress at 2.5×10^6 cycles of life.

The distributional Goodman diagrams of figure 5, for 2.5×10^6 cycles of life, show that there is little effect on the alternating bending strength mean at stress ratios greater than 1.0, due to the superimposition of constant torsion onto alternating bending stress. However, there is an increasingly sharp reduction in the alternating bending strength as the stress ratio decreases below 1.0. It appears that the added shear stress is asserting its influence when its nominal stress level is higher than about 230 MN/m^2 (33 ksi). Furthermore, figure 5(a) indicates that there is a substantial increase in the standard deviation of the failure governing strength distribution as the stress ratio decreases below 1.0 and that the standard deviation reaches a maximum at a stress ratio of about 0.30. Thereafter, it drops sharply and converges to its minimum at $\bar{r} = 0$, which is the standard deviation of the static ultimate tensile strength distribution.

CONCLUDING REMARKS

The abscissas in figure 5 show the static ultimate tensile strength of the ungrooved specimens because this is the most commonly available static strength information. A Goodman diagram analysis using the static ultimate strength distribution of the grooved specimens has been programmed. Further, nominal alternating bending strength has been used throughout to represent the alternating strength. There are two reasons for this: (1) The actual bending and shear stresses at the base of the test specimen groove are not known because the exact fatigue stress concentration factor for this material under combined bending torsion is not known. (2) Normally in design, the nominal bending and shear stresses are calculated first, and, to determine the corresponding fatigue strength distribution, the designer need only enter figures 5(a) or (b) with these nominal stresses.

The design application presented in this study provides a vivid illustration of the great value of this research. It shows how to calculate the reliability of shafts subjected to a variety of loading conditions by the design-by-reliability methodology. The calculated reliability provides an explicit quantitative measure of the design integrity that no other method can provide. The 40-percent weight savings achieved by the design-by-reliability methodology over that of the conventional design methodology in the design example for the same reliability dramatizes the value of the methodology and of the experimental, distributional S-N, and Goodman diagram design data generated by this research.

Lewis Research Center,
National Aeronautics and Space Administration,
Cleveland, Ohio, August 1, 1974,
120-60.

APPENDIX A

DETERMINISTIC SHAFT DESIGN

The shaft shown in figure 15 supports an alternator rotor. It is to be made of AISI 4340 steel, heat treated to a Brinell hardness of 323 to 370 (R_C 35 to 40) with a ground finish. The rotor will subject the shaft to a radial bending load of 607.4 newtons (136.8 lb) and a torque of 112 newton-meters (1000 lb-in.) when delivering full-load electrical power. The spline drive may exert a maximum misalinement radial force of 13.3 newtons (3 lb). The temperature to be experienced by the shaft will be 294 to 300 K (70° to 80° F). The shaft will rotate at 12 000 rpm and have a life of 2.5×10^6 cycles with a reliability of 0.999.

What should the shaft's diameter be using the conventional deterministic design methodology?

Solution: Various methods can be used for machine design problems in which the shaft diameter is unknown. For aerospace applications weight, life, and reliability are important considerations. Shigley (ref. 16, p. 482) has shown that under these conditions it is wise to use the von Mises-Hencky-Goodman method. This method requires knowledge of material strengths and application stresses. Table A-3 of reference 32 (p. 564) gives the tensile properties for 2.54-centimeter (1-in.) round, drawn condition, 277 Brinell hardness material as $S_y = 1103$ MN/m^2 (or 160 ksi) and $S_{ut} = 1289$ MN/m^2 (or 187 ksi).

According to Juvinall (ref. 32, pp. 236-256) the endurance limit S_n may be found using modifying factors as follows:

$$S_{n_{10^6}} = \frac{S'_n C_L C_D C_S}{K_f} \tag{34}$$

where

$$S'_n = 0.50\, S_{ut} = 644.6 \text{ MN/m}^2 \text{ (or 93.5 ksi)}$$

when $S_{ut} = 1379$ N/m^2 (200 ksi; ref. 32, p. 211), and where the type of load C_L is 1.0 for reverse bending (ref. 32, p. 231), the effect of size C_D is 0.9 for specimens up to 5.08 centimeters (2 in.; ref. 32, p. 232), the effect of surface C_S is 0.88 for a ground finish (ref. 32, p. 234), and the fatigue stress concentration factor K_f is (ref. 32, p. 257)

$$K_f = 1 + (K_t - 1)qC_S \tag{38}$$

The maximum theoretical shear and bending stress concentration factor at this shoulder are (ref. 34, pp. 75-76)

$$K_s = 1.19 \qquad \text{and} \qquad K_b = 1.30$$

for a shaft around 1.27 centimeters (1/2 in.) in diameter with a 0.318-centimeter shoulder radius. What to do when stress concentration is caused by a combined bending-torsion load has not been adequately investigated, but it is reasonable that the combined effect would be no greater than the product of each factor; therefore,

$$K_t = (1.19)(1.30) = 1.55$$

Notch sensitivity q, based on data (ref. 33, pp. 296-298) for a notch radius of 0.318 centimeter (0.125 in.) and $S_{ut} = 1289\ MN/m^2$ (187 ksi), is 0.90. Therefore, the maximum fatigue stress concentration factor from equation (38) is

$$K_f = 1 + (1.55 - 1)(0.90)(0.88) = 1.43$$

From equation (34)

$$S_n = \frac{644.6(1.0)(0.90)(0.88)}{1.43} = 357.1\ MN/m^2 \text{ (or 51.8 ksi)}$$

To satisfy the reliability specification, an additional modifying factor K_c (ref. 16, p. 169) must be introduced. From Shigley (ref. 16, p. 169) K_c is determined as

$$K_c = 1 - 0.008\,D = 0.75$$

The resulting endurance limit now becomes

$$S_{n,\,corr} = K_c S_n = (0.75)(357.1) = 268.9\ MN/m^2 \text{ (or 39.0 ksi)}$$

The bending moment M at the shoulder is 14.1 meter-newtons (126 in.-lb). The bending stress $\sigma_{x,\,a}$ at the shoulder is calculated from[3]

$$\sigma_{x,\,a} = \frac{Mc}{I} = \frac{14.1}{\pi d^3/32} = \frac{144}{d^3} \qquad \left(\text{or } \frac{1280}{d^3}\right) \tag{39}$$

[3]Parentheticals contain U. S. Customary values.

The torque T is constant over the shaft length at 113 newton-meters (1000 lb-in.). The torsional stress $\tau_{xz,m}$ in the design section of the shaft is

$$\tau_{xz,m} = \frac{Tc}{J} = \frac{113}{\pi d^3/16} = \frac{576}{d^3} \qquad \left(\text{or } \frac{5100}{d^3}\right) \tag{40}$$

From the von Mises-Hencky failure criterion, given by equations (5), (9), and (10), the failure governing mean shear stress $\tau_{xz,m}$ is maximum at the outer fiber of the shaft at which point the contribution due to the vertical shear of the specimen is zero and therefore, is not included in the analysis. Thus, the von Mises-Hencky stress components using equations (9) and (10) become

$$s_a = \sigma_{x,a} = \frac{144}{d^3} \qquad \left(\text{or } \frac{1280}{d^3}\right) \tag{41}$$

and

$$s_m = \sqrt{3}\,\tau_{xz,m} = \frac{998}{d^3} \qquad \left(\text{or } \frac{8830}{d^3}\right) \tag{42}$$

and equation (5) becomes

$$r = \frac{s_a}{s_m} = 0.144 \tag{43}$$

A conventional Goodman diagram can be prepared from these data. The alternating and mean stresses are plotted as ordinate and abscissa, respectively, in figure 16. Defining stress-to-failure as material strength makes it possible to use the Goodman boundary to represent the strength of this material as modified by environmental factors. The top portion of the Goodman boundary (line 1) is obtained by drawing a straight line between the ordinate at S_n = 269 MN/m^2 (39 ksi) and the abscissa at S_{ut} = 1289 MN/m^2 (187 ksi). The right boundary (line 2) is defined by a straight line joining the ordinate at S_y = 1103 MN/m^2 (160 ksi) with the abscissa also at S_y = 1103 MN/m^2 (160 ksi). A third straight line (line 3) is constructed to define S_a and S_m, for this case, with $\tan\theta = 0.144 \times 6 = \tan 40.8$. (The factor of 6 takes into account the fact that the abscissa scale is 6 times that of the ordinate scale.) The intersection of lines 1 and 3 define the point S_a = 109.6 MN/m^2 (15.9 ksi) and S_m = 762.5 MN/m^2 (110.6 ksi).

In conventional design a margin of safety of at least 100 percent is used to insure a no failure design. This requires that s_a be constrained as follows:

$$s_a \leq \frac{S_a}{2} = \frac{109.6}{2} \qquad \left(\text{or } \frac{15.9}{2}\right) \tag{44}$$

Substitution of equation (41) into equation (44) yields

$$\frac{144}{\bar{d}^3} \leq 54.8 \qquad \left(\text{or } \frac{1280}{\bar{d}^3} \leq 7.95 \times 10^3\right) \tag{45}$$

Then

$$\bar{d}^3 \geq \frac{144}{54.8} = 2.627 \qquad \left(\text{or } \frac{1280}{7950} = 0.161\right) \tag{46}$$

or

$$\bar{d} \geq 1.38 \text{ cm} \qquad (\text{or } 0.544 \text{ in.})$$

Based on these results a shaft diameter of at least 1.39 centimeters (35/64 in.) should be recommended. The inputs and results of the conventional deterministic design methodology are summarized in table IX for purposes of comparison with the results of the design-by-reliability methodology, which is discussed in appendix B.

APPENDIX B

SHAFT DESIGN BY RELIABILITY

Now let the alternator shaft of appendix A be designed using the reliability approach to rotating component design.

Solution: To design by reliability, data in the form of the distributional Goodman diagram given in figure 5(a) must be used. The design-by-reliability methodology has been detailed in a previous paper (ref. 1). The shaft is to be made of AISI 4340 steel, heat treated to Rockwell C hardness 35 to 40 or Brinell hardness 323 to 370. Figure 5(a) provides the fatigue strength data required.

Since the research has generated data for the strength of the material desired under combined conditions of reversed bending and steady torque for various stress ratios, the modifying factors required by Juvinall in appendix A, namely, C_D and C_S are already included in the data. The reliability factor K_c is introduced differently in the design-by-reliability methodology, as will be shown later. The difference in K_f for this shaft and the research specimens is negligible. All other modifying factors are taken to be unity as in appendix A.

The bending moment at the shoulder is taken to be normally distributed[1] with parameters (14. 1; 1. 58) meter-newtons ((126; 11. 4) in. -lb). The failure governing stress s_a at the shoulder is calculated from equation (13). The distribution parameters of s_a, taken to be normal, are found using equation (13) and the method of binary synthesis of normal distributions (ref. 38, pp. 279-282 and table 9), such that

$$\bar{s}_a = 10.2 \frac{\overline{M}}{\bar{d}^3} \tag{47}$$

and

$$\sigma_{s_a} = \frac{10.2}{\bar{d}^3} \left\{ \frac{M^2 \sigma^2_{\bar{d}^3} + \left[d^3 \right]^2 \sigma^2_M}{\left[\bar{d}^3 \right]^2 + \sigma^2_{\bar{d}^3}} \right\}^{1/2} \tag{48}$$

where

[1]Normal distribution notation (mean; standard deviation).

$$\sigma_{d^3} = 3\,\bar{d}^{\,2}\sigma_d = 3\,\bar{d}^{\,2}(0.015\,\bar{d}) = 0.045\,\bar{d}^{\,3}$$

and where σ_d is taken to be 1/6 of the total specified tolerance, or $0.015\,\bar{d}$, $\overline{M} = 14.1$ meter-newtons (126 in. -lb) and $\sigma_M = 1.58$ meter-newtons (11.4 in. -lb). (This has to be specified.) Substitution of these quantities into equations (47) and (48) yields

$$\bar{s}_a = 10.2\,\frac{14.1}{\bar{d}^{\,3}} = 144\,\frac{1}{\bar{d}^{\,3}} \qquad \left(\text{or } \frac{1280}{\bar{d}^{\,3}}\right) \tag{49}$$

and

$$\sigma_{s_a} = \frac{10.2}{\bar{d}^{\,3}}\left\{\frac{(14.1)^2\left[0.045\,\bar{d}^{\,3}\right]^2 + \bar{d}^{\,6}(1.58)^2}{\bar{d}^{\,6} + (0.045\,\bar{d}^{3})^2}\right\}^{1/2} = 14.7\,\frac{1}{\bar{d}^{\,3}} \qquad \left(\text{or } \frac{129.7}{\bar{d}^{3}}\right) \tag{50}$$

The distribution parameters of s_m, taken to be normal, are found similarly from equation (42) as follows:

$$\bar{s}_m = 8.83\,\frac{\overline{T}}{\bar{d}^{\,3}} \tag{51}$$

and

$$\sigma_{s_m} = \frac{8.83}{\bar{d}^{\,3}}\left\{\frac{\overline{T}^{\,2}\sigma^2_{\bar{d}^{\,3}} + \left[\bar{d}^{3}\right]^2\sigma^2_T}{\left[\bar{d}^{3}\right]^2 + \sigma^2_{\bar{d}^{3}}}\right\}^{1/2} \tag{52}$$

where

$$\overline{T} = 113 \text{ N-m (or 1000 lb-in.)}$$

and

$$\sigma_T = 9 \text{ N-m (or 80 lb-in.)}$$

Substitution of these quantities into equations (51) and (52) yields

$$s_m = 8.83 \frac{112}{\bar{d}^3} = \frac{998}{\bar{d}^3} \qquad \left(\text{or } \frac{8830}{\bar{d}^3}\right) \tag{53}$$

and

$$\sigma_{s_m} = \frac{8.83}{\bar{d}^3}\left\{\frac{(113)^2\left[0.045\,\bar{d}^3\right]^2 + \bar{d}^6(9)^2}{\bar{d}^6 + (0.045\,\bar{d}^3)2}\right\}^{1/2} = \frac{91.5}{\bar{d}^3} \qquad \left(\text{or } \frac{810}{\bar{d}^3}\right) \tag{54}$$

From equations (50), (54), and (43)

$$r = \frac{s_a}{s_m} = \frac{\frac{144}{\bar{d}^3}}{\frac{998}{\bar{d}^3}} = 0.144 \tag{55}$$

(It is assumed that the variability of r will not affect the reliability significantly.) The two stresses, s_a and s_m, must now be synthesized into the failure governing stress distribution $f(s_f)$, along the stress ratio line $\bar{r} = 0.144$, equations (7) and (8), as follows:

$$\bar{s}_f = \bar{s}_a\left(1 + \frac{1}{\bar{r}^2}\right)^{1/2} \tag{56}$$

and

$$\sigma_{s_f} = \sigma_{s_a}\left(1 + \frac{1}{\bar{r}^2}\right)^{1/2} \tag{57}$$

In equation (56) $\bar{s}_a$ is obtained from equation (49) and $\bar{r} = 0.144$. And in equation (57) $\sigma_{s,a}$ is obtained from equation (50). Substitution of these in equations (56) and (57) yields

$$\bar{s}_f = 144 \frac{1}{\bar{d}^3}\left(1 + \frac{1}{(0.144)^2}\right)^{1/2} = 144 \frac{1}{\bar{d}^3}(7.016) = 1010 \frac{1}{\bar{d}^3} \quad \left(\text{or } \frac{9016}{\bar{d}^3}\right) \tag{58}$$

Similarly,

$$\sigma_{s_f} = 14.7 \frac{1}{\bar{d}^3}\left(1 + \frac{1}{(0.144)^2}\right)^{1/2} = 14.7 \frac{1}{\bar{d}^3}(7.016) = 103 \frac{1}{\bar{d}^3} \quad \left(\text{or } \frac{910}{\bar{d}^3}\right) \tag{59}$$

Thus the mean and the standard deviation of the failure governing stress distribution have been determined.

The next step is to determine the failure governing strength distribution parameters. Since the design strength data presented in figure 5(a) apply to this case for $r = 0.144$. Figure 5(a) yields

$$\bar{S}_f = 1213 \text{ MN/m}^2 \text{ (176 ksi)}$$

and

$$\sigma_{S_f} = 46.4 \text{ MN/m}^2 \text{ (6.73 ksi)}$$

If the failure governing strength distribution $f(S_f)$ and the failure governing stress distribution $f(s_f)$ are taken to be normal, then these two distributions can be coupled to obtain with the reliability of these shafts as follows (ref. 1, pp. 556-557):

$$\mathscr{R} = \int_{-(\bar{\xi}/\sigma_\xi)}^{+\infty} f(z)dz \tag{60}$$

where

$$-(\zeta/\sigma_\zeta) = \frac{\bar{s}_f - \bar{S}_f}{\left(\sigma^2_{s_f} + \sigma^2_{S_f}\right)^{1/2}} \tag{61}$$

As the specified shaft reliability is 0.999, the value of z(f) may be found to be -3.09 from the standardized normal distribution probability tables. Consequently, using this value and the values of the previously determined parameters of $f(s_f)$ and $f(S_f)$, equation (61) yields

$$-3.09 = \frac{1010\,\frac{1}{\bar{d}^3} - 1213}{\left\{\left[103\,\frac{1}{\bar{d}^3}\right]^2 + (46.4)^2\right\}^{1/2}} \tag{62}$$

Rearrangement of equation (62) yields

$$\bar{d}^{\,6} - 1.6885\,\bar{d}^{\,3} + 0.6332 = 0 \tag{63}$$

and solving for the roots of equation (63) yields a mean shaft diameter of $\bar{d} = 1.04$ centimeter (0.411 in.). Consequently, the use of $d = 1.07$ centimeter (27/64 in.) would be recommended, as compared with a diameter of $d = 1.39$ centimeters (or 35/64 in.) required by the conventional, deterministic design.

The inputs, outputs, and results for both design methodologies are given in table IX. An a priori reliability is designed into the shaft through the design-by-reliability methodology, which results in a better than 40-percent saving in material for this case. Furthermore, the design integrity is known in terms of a reliability of 0.999, such that on the average no more than one in 1000 such shafts will fail while performing a mission of 2.5×10^6 cycles duration. If a higher reliability is desired, the corresponding value for $-(\bar{\zeta}/\sigma_\zeta)$ can be found, and the required shaft diameter recalculated by the design-by-reliability methodology. Since all design variables are explicitedly brought into this methodology and incorporated into the failure governing stress and strength distributions to enable the determination of the designed-in reliability, the design can be optimized from the point of view of shaft geometry, loads, and material strength

characteristics. This example thus vividly illustrates the great value of the probabilistic design-by-reliability methodology of designing rotating shafts subjected to combined reversed bending and steady torque loads.

APPENDIX C

THE ALGEBRA OF NORMAL FUNCTIONS

The algebra of normal functions is a useful method of performing mathematical operations with statistical functions (ref. 8). This method is primarily intended for use in the probabilistic design-by-reliability approach. All variables are assumed to be normally distributed; the mathematical operations for the sum, difference, product, and quotient of two normal random variables are also assumed to be normally distributed. (This is only valid for the sum and difference of two normally distributed random variables.) Under these conditions, an algebra can be developed to facilitate mathematical operations required in design. The mathematical operations of this algebra are summarized in table X. Some variables that are important in the design-by-reliability method are not normally distributed. To handle these design variables other methods, such as the Monte Carlo (ref. 39 or 40) and the system moments (ref. 40, pp. 228-235), are available.

REFERENCES

1. Kececioglu, Dimitri; and Cormier, David: Designing a Specified Reliability Directly into a Component. Proc. Third Annual Aerospace Reliability and Maintainability Conf. SAE, 1964, pp. 546-565.

2. Freudenthal, A. M.: Safety, Reliability and Structural Design. Am. Soc. of Civil Eng. Trans., pt. II, vol. 127, 1962, pp. 304-323.

3. Freudenthal, Alfred M.; Garrelts, Jewell M.; and Shinozuka, Mosanober: The Analysis of Structural Safety. ASCE Structural Div. J., vol. 92, Feb. 1966, pp. 267-325.

4. Mittenbergs, A. A.: Fundamental Aspects of Mechanical Reliability. Mechanical Reliability Concepts. ASME, 1965, pp. 17-34.

5. Clover, A. H.; Rosenfield, A. R.; Putnam, A. A.; Mesloh, R. E.; Cassidy, L. M.; Simon R.; and Mittenbergs, A. A.: Probabilistic Design of Mechanical Components. Battelle Memorial Institute, 1965.

6. Bush, Thomas L.; Meyers, Anthony P.; and Simonaitis, Darwin F.: Methods for Prediction of Electro-Mechanical System Reliability. Rep. 2, IIT Research Institute, May 1965. (Available for DDC as AD-474907.)

7. Bratt, M. J.; Reethof, G.; and Weber, G. W.: A Model for Time Varying and Interferring Stress-Strength Probability Density Distributions with Consideration for Failure Incidence and Property Degradation. Proc. Third Annual Aerospace Reliability and Maintainability Conf., SAE, pp. 566-575, 592.

8. Haugen, Edward B.: Probabilistic Approaches to Design. John Wiley and Sons, 1968.

9. Kececioglu, Dimitri:, McKinley, J. W.; and Saroni, M. J.: A Probabilistic Method of Designing Specified Reliabilities into Mechanical Components with Time Dependent Stress and Strength Distributions. University of Arizona (NASA CR-72836), 1967, p. 331.

10. Kececioglu, Dimitri; et al.: Design, Development and Results from Combined Bending-Torsion Fatigue Reliability Research Machines. Univ. Arizona (NASA CR-72838), 1969.

11. Kececioglu, Dimitri; and Broome, H. Wilson: Probabilistic-Graphical Phenomenological Analysis of Combined Bending-Torsion Fatigue Reliability Data. Univ. Arizona (NASA CR-72839), 1969.

12. Kececioglu, Dimitri; and McConnell, J. B.: Calibration of Combined Bending Torsion Fatigue Reliability Research Machines and Reliability Data Reduction. University of Arizona (NASA CR-72839), 1969, p. 151.

13. Kececioglu, Dimitri; and Smith, John L.: Statistical Complex Fatigue Data for SAE 4340 Steel and its Use in Design by Reliability. Univ. Arizona (NASA CR-72835), 1970.

14. Kececioglu, Dimitri; and Guerrieri, William N.: Generation of Finite Life Distributional Goodman Diagrams for Reliability Prediction. The Univ. Arizona, (NASA CR-120813), Aug. 3, 1971.

15. Kececioglu, Dimitri; and Chester, Louie B.: Modern Methodology of Designing Target Reliability into Rotating Mechanical Components. Arizona University (NASA CR-120967), 1973.

16. Shigley, Joseph E.: Mechanical Engineering Design. McGraw-Hill Book Co., Inc., 1963.

17. Lipson, Charles; and Juvinall, R. C., eds.: Application of Stress Analysis to Design and Metallurgy. Univ. Michigan Summer Conf., Ann Arbor, Mich., 1961.

18. Marin, Joseph: Design for Fatigue Loading. Machine Design, vol. 29, no. 4, Feb. 21, 1957, pp. 124-133.

19. Springer, M. D.; and Thompson, W. E.: The Distribution of Products of Independent Random Variables. Rep. TR64-46, General Motors Corp., Aug. 1964. (Available from DDC as AD-447393.)

20. Donahue, James D.: Products and Quotients of Random Variables and Their Applications. Martin Co. (ARL-64-115, AD-603667), July 1964.

21. Shreĭder, Yu. A.: The Monte Carlo Method; The Method of Statistical Trials. Pergamon Press, 1966.

22. Curtiss, J. H.: Monte Carlo Methods for the Weration of Linear Operators. Rep. 2365, National Bureau of Standards, 1953.

23. Meyer, Herbert A.: Symposium on Monte Carlo Methods. John Wiley & Sons, Inc., 1956.

24. Lalli, V. R.; and Vargo, D. J.: Aerospace Reliability Applied to Biomedicine. NASA TM X-67942, 1971.

25. Kececioglu, Dimitri; Smith, Richard E.; and Felsted, Ernest A.: Distributions of Strength in Simple Fatigue and the Associated Reliabilities. Annals of Reliability and Maintainability. Vol. 9. SAE, 1970, pp. 659-672.

26. Dixon, W. J.; and Mood, A. M.: A Method for Obtaining and Analyzing Sensitivity Data. J. Am. Stat. Assoc., vol. 43, no. 241, 1948, pp. 109-126.

27. Timoshenko, Stephen: Strength of Materials. Part II. Third ed., D. Van Nostrand Co., 1956, pp. 438-558.

28. Jailer, Robert W.; Freilich, Gerald; and Castellon, Angelo W.: Flight Vehicle Power Systems Reliability Criteria. Rep. APJ-268-1, American Power Jet Co., Ridgefield, New Jersey, 1962.

29. Mabie, H. H.; and Gjesdahl, M. S.: A Fatigue Testing Machine for Reversed Bending and Steady Torque. Proc. Soc. Experimental Stress Analysis. vol. 14, no. 1, C. V. Mahlmann and W. M. Murray, eds., 1956, pp. 83-88.

30. Lalli, Vincent R.; and Kececioglu, Dimitri: An Approach to Reliability Determination of a Rotating Component Subject to Complex Fatigue. Annals of Reliability and Maintainability. Vol. 9. SAE, 1970, pp. 534-548.

31. A Guide for Fatigue Testing and the Statistical Analysis of Fatigue Data. Second ed. Spec. Tech. Publ. No. 91-A, ASTM, 1963.

32. Juvinall, Robert C.: Engineering Considerations of Stress, Strain, and Strength. McGraw-Hill Book Co., Inc., 1967.

33. Sines, George; and Waisman, J. L., eds.: Metal Fatigue. McGraw-Hill Book Co., Inc., 1959.

34. Peterson, Rudolph E.: Stress Concentration Design Factors. John Wiley & Sons, Inc., 1953.

35. Kececioglu, Dimitri; Smith, Richard E.; and Felsted, Ernest A.: Distributions of Cycles-to-Failure in Simple Fatigue and the Associated Reliabilities. Annals of Assurance Sciences. Gordon and Breach Science Publ., 1969, pp. 357-374.

36. Kececioglu, Dimitri; and Haugen, Edward B.: A Unified Look at Design Safety Factors, Safety Margins, and Measures of Reliability. Annals of Assurance Sciences. ASME, 1968, pp. 520-530.

37. Kececioglu, Dimitri; and Haugen, Edward B.: Fatigue Reliability Design Data for Dynamic and Rotary Machinery. Space Systems and Thermal Technology for the 70's. Part 1. ASME, 1970.

38. Kececioglu, Dimitri: Reliability Analysis of Mechanical Components and Systems. Nuclear Engineering and Design. North Holland Publishing Co., 1972, pp. 259-290.

39. Hahn, G. J.; and Shapiro, S. S.: Statistical Models in Engineering. John Wiley & Sons, Inc., 1967.

TABLE I. - COMBINED BENDING AND SHEAR STRESS LEVELS

Stress ratio			Nominal alternating bending stress				Nominal shear stress				Nominal normal mean stress[b]				Sample size, n
Average, $\bar{r}$ (a)	Standard deviation, σ_r	$\sigma_r/\bar{r}$	s_a		Standard deviation, σ_{s_a}		$\bar{\tau}_{xz,m}$		Standard deviation, $\sigma_{\tau_{xz,m}}$		s_m		Standard deviation, σ_{s_m}		
			MN/m^2	ksi	MN/m^2	ksi	MN/m^2	ksi	MN/m^2	ksi	MN/m^2	ksi	MN/m^2	ksi	
Phase I															
∞	(c)	(c)	992.7	144.0	10.3	1.5	0	0	0	0	----	-----	----	---	12
			785.9	114.0	6.2	.9					----	-----	----	---	18
			675.6	98.0	18.6	2.7					----	-----	----	---	
			561.9	81.5	6.2	.9									
			503.3	73.0	12.4	1.8					----	-----	----	---	
3.5	0.14	0.04	1041.0	151.0	26.2	3.8	172.4	25.0	5.5	0.8	----	-----	----	---	12
	.14	.04	789.4	114.5	12.4	1.8	134.4	19.5	4.8	.7	----	-----	----	---	18
	.18	.05	572.2	83.0	8.3	1.2	93.1	13.5	4.8	.7	----	-----	----	---	18
	.17	.05	510.2	74.0	5.5	.8	86.2	12.5	4.1	.6	----	-----	----	---	18
0.83	0.03	0.03	765.2	111.0	8.7	1.3	506.7	73.5	14.5	2.1	----	-----	----	---	12
	.08	.10	627.3	91.0	46.2	6.7	458.5	66.5	24.1	3.5	----	-----	----	---	18
	.07	.09	520.5	75.5	22.1	3.2	363.8	53.5	23.4	3.4	----	-----	----	---	18
	.06	.08	448.1	65.0	26.9	3.9	324.0	47.0	8.7	1.3	----	-----	----	---	18
0.44	0.01	0.02	475.7	69.0	9.6	1.4	620.5	90.0	5.5	0.8	----	-----	----	---	18
	.01	.02	444.7	64.5	8.7	1.3	586.0	85.0	12.4	1.8	----	-----	----	---	18
	.01	.02	413.6	60.0	4.8	.7	541.2	78.5	9.6	1.4	----	-----	----	---	18
Phase II															
∞	(c)	(c)	750.8	108.9	8.7	1.3	0	0	0	0	0	0	0	0	35
			634.9	92.1	4.8	.7	0	0	0	0	0	0	0	0	35
			507.4	73.6	5.5	.8	0	0	0	0	0	0	0	0	35
1.06	0.02	0.02	728.7	105.7	8.7	1.3	895.7	57.4	5.5	0.8	682.4	99.0	9.6	1.4	35
	.01	.01	587.4	85.2	4.1	.6	321.9	46.7	2.8	.4	558.3	81.0	4.1	.6	
	.01	.01	447.4	64.9	3.4	.5	243.4	35.3	1.4	.2	420.5	61.0	2.8	.4	
	.01	.01	277.1	40.2	1.4	.2	150.3	21.8	1.4	.2	255.0	37.0	2.8	.4	
0.40	0.01	0.03	342.6	49.7	6.2	0.9	517.7	71.5	9.6	1.4	853.4	123.8	16.5	2.4	35
	.01	.03	275.8	40.0	4.1	.6	396.4	57.5	6.9	1.0	685.9	99.5	11.7	1.7	35
	0	0	242.0	35.1	1.4	.2	346.8	50.3	2.8	.4	599.7	87.0	5.5	.8	35
0.25	0	0	273.0	39.6	2.8	0.4	635.6	92.2	5.5	0.8	1100.8	159.7	9.6	1.4	35
	0	0	241.3	35.0	2.1	.3	559.1	81.1	7.6	1.1	968.5	140.5	13.1	1.9	35
0.15	0	0	220.3	32.0	3.4	0.5	849.3	123.2	8.3	1.2	1470.9	213.4	13.8	2.0	37
	0	0	188.9	27.4	2.8	.4	732.8	106.3	10.3	1.5	1269.0	184.1	17.9	2.6	35
	0	0	179.2	26.0	2.1	.3	691.5	100.3	8.3	1.2	1197.3	173.7	13.8	2.0	35

[a] $\bar{r} = \bar{s}_a / \sqrt{3}\,\bar{\tau}_{xz,m}$.

[b] $\bar{S}_m = \sqrt{3}\,\tau_{xz,m}$, using von Mises-Hencky failure theory, and $\sigma_{S_m} = \sqrt{3}\,\sigma_{\tau_{xz,m}}$.

[c] Not applicable.

TABLE II. - SUMMARY OF ENDURANCE STRENGTH RESULTS FOR

DISTRIBUTIONAL GOODMAN DIAGRAM

[2.5×10^6 cycles of life, AISI 4030 steel, R_c 35 to 40; grooved specimens.]

Stress ratio, $\bar{r}$	Nominal alternating bending strength				Nominal shear strength[a]				Nominal combined strength vector[b]			
	$\bar{S}_a$		Standard deviation, $\bar{\sigma}_{S_a}$		$\bar{\tau}_{xz,m}$		Standard deviation, $\sigma_{\tau_{xz,m}}$		$\bar{S}_v$		Standard deviation, σ_{S_v}	
	MN/m^2	ksi	MN/m^2	ksi	MN/m^2	ksi	MN/m^2	ksi	MN/m^2	ksi	MN/m^2	ksi
Phase I												
∞	395.0	57.3	20.0	2.9	0	0	0	0	395.0	57.3	20.0	2.9
3.5	379.9	55.1	25.5	3.7	108.2	15.7	7.6	1.1	395.0	57.3	26.9	3.9
1.0	384.7	55.8	22.8	3.3	391.6	56.8	22.8	3.3	543.9	78.9	32.4	4.7
.45	341.9	49.6	25.5	3.7	759.7	110.2	56.5	8.2	833.5	120.9	62.0	9.0
Phase II												
∞	232.3	33.7	18.6	2.7	0	0	0	0	232.3	33.7	18.6	2.7
1.06	220.6	32.0	19.3	2.8	208.2	30.2	17.9	2.6	303.3	44.0	26.2	3.8
.40	209.6	30.4	20.0	2.9	523.9	76.0	49.6	7.2	564.6	81.9	53.8	7.8
.25	166.1	24.1	11.7	1.7	665.3	96.5	47.6	6.9	686.0	99.5	48.9	7.1
.15	157.9	22.9	4.8	.7	1052.7	152.7	32.4	4.7	1064.4	154.4	32.4	4.7

[a] $\bar{\tau}_{xz,m} = \dfrac{\bar{S}_a}{\sqrt{3}\,\bar{r}}$ and $\sigma_{\tau_{xz,m}} = \dfrac{1}{\sqrt{3}\,\bar{r}}\sigma_{S_a}$.

[b] $\bar{S}_v = \bar{S}_a\left(1 + \dfrac{1}{\bar{r}^2}\right)^{1/2}$ and $\sigma_{S_v} = \sigma_{S_a}\left(1 + \dfrac{1}{\bar{r}^2}\right)^{1/2}$

TABLE III. - OPERATIONAL SPECIFICATIONS FOR THE COMBINED-STRESS FATIGUE RESEARCH MACHINES

Component	Description
Test machine[a]	Accommodate a specimen rotating at 1800 rpm; produce and hold a steady torque and a reversed bending moment; holding chuck, 2.5-cm-diam maximum; simple design employing "off-the-shelf" components.
Loading mechanism for steady torque	Simple device to produce, hold, and transmit desired steady torque of 605 N-m (5400 lb-in.) to test specimen.
Loading mechanism for reversed bending	Simple device to produce a reversed bending moment of 386 m-N (3450 in. -lb) while specimen is rotating
Test specimen	AISI 4340 steel, condition C-4; MIL-S-5000B, certification of chemical and physical properties; uniform quality, same heat and processing, heat treat to Rockwell C 35 to 40 as per MIL-H-6875 with minimum tempering temperature of 540° C; inspection as per MIL-I-6868; D = 1.87 cm, d = 1.27 cm, r = 0.38 cm; K_b = 1.45; K_s = 122 with 2.5 by 0.32 cm keyway.
Instrumentation -	
Strain gages	To obtain dynamic and static strain measurements in bending and torsion.
Channels	To handle at least six sets of strain gage output simultaneously.
Slip rings	To transfer strain gage data to amplifier while specimen is rotating.
Amplifier	To amplify static and dynamic output from strain gages.
Recorder	To produce a permanent record of amplified strain gage outputs.

[a]Three such machines have been built and are being used to obtain distributional combined stress fatigue data for the steel specimens specified above.

TABLE IV. - MODE 5[a] CALIBRATION COEFFICIENTS

Machine	Calibration coefficient[a, b]					Machine speed, rpm
	Bending in groove, $\mathscr{K}_{BGR}$	Groove to tool holder, $\mathscr{K}_{GRTH}$	Tool holder torque, $\mathscr{K}_{T}$	Torque interaction into bending, $\mathscr{K}_{T/B}$	Bending interaction into torque, $\mathscr{K}_{B/T}$	
1	1.3081	0.0149	0.8753	-0.0462	0.0477	1779
2	1.3081	.0145	.8950	.0463	.0555	1775
3	1.3081	.0170	.8748	.0542	.0645	1778

[a]Mode 5 operation refers to the computer program code that identifies the proper set of calibration coefficients to be used with each set of machine data obtained during a specific calendar period.

[b]These calibration constants are traceable to the National Bureau of Standards standards.

TABLE V. - TYPICAL ENDURANCE STRENGTH

DATA PROCESSING[a]

[AISI 4340 steel; Rockwell C, 35 to 40; stress ratio ratio, 0.44; grooved specimen. See fig. 1. Test was considered a success if specimens did not break in 2.5×10^6 cycles (see fig. 21).]

Alternating strength, $\bar{S}_a$		i (level)	n_i (successes)	in_i	i^2n_i
MN/m^2	ksi				
370	53.7	3	3	9	27
350	50.8	2	8	16	32
330	47.9	1	7	7	7
310	45.0	0	3	0	0
Totals:			n = 21,	A = 32,	B = 66

[a]A calculation of the mean and standard deviation using the staircase method is

$d_i = 20.0\ MN/m^2$ (2.9 ksi)

$S_o = 310\ MN/m^2$ (45.0 ksi)

$$\mu_{S_a} = s_o + d_i\left(\frac{A}{N} + \frac{1}{2}\right) = 31.0 + 2.0\left(\frac{32}{21} + \frac{1}{2}\right) = 350\ MN/m^2$$ (50.8 ksi)

$$\sigma_{S_a} = 1.620\ d\left(\frac{NB - A^2}{N^2} + 0.029\right) = 1.620 \times 2.0 \times \left[\frac{21 \times 66 - (32)^2}{(21)^2} + 0.029\right] = 29\ MN/m^2\ (4.2\ ksi)$$

A summary of the mean and standard deviation endurance strength estimates are given in table II.

TABLE VII. - LIFE DISTRIBUTION PARAMETERS FOR PHASE I RESULTS

Stress ratio, $\bar{r}$	Alternating stress, $\bar{s}$		Sample size, n	Life, kilocycles		Skewness, α_3	Kurtosis, α_4	K-S test difference, D (a)	Life, $\log_e$ kilocycles		Skewness, α_3	Kurtosis, α_4	K-S test difference, D (a)
	MN/m^2	ksi		$\bar{N}_f$	σ_{N_f}				$\bar{N}_f$	α_{N_f}			
				Normal distributions					Log-normal distributions				
∞	696.3	101.0	12	2.8	0.53	-1.344	3.561	0.175	7.907	0.228	-1.586	4.258	0.207
	551.5	80.0	18	9.0	1.02	-.247	1.995	.099	9.102	.114	-.407	2.123	.092
	475.7	69.0	↓	22.2	3.82	-.042	1.855	.082	9.992	.176	-.265	1.945	.094
	396.4	57.5		78.0	12.55	.873	3.060	.184	11.252	.154	.575	2.697	.159
	355.0	51.5		162.0	34.39	-.616	2.201	.174	11.971	.235	-.906	2.707	.198
3.5	730.8	106.0	12	1.5	0.28	-0.222	1.725	0.113	7.262	0.198	-0.435	2.006	0.128
	550.0	80.5	18	6.2	1.01	.797	3.397	.111	8.721	.157	.403	2.869	.086
	403.3	58.5	18	39.6	12.99	1.876	7.241	.239	10.545	.287	.686	4.407	.184
	358.5	52.0	18	74.2	19.53	.147	2.057	.132	11.180	.274	-.342	2.501	.084
0.83	537.7	78.0	12	6.6	1.01	9.893	2.493	[b]0.296	8.778	0.146	0.742	2.295	[c]0.280
	444.7	64.5	18	20.5	5.59	.239	2.257	.119	9.890	.281	-.171	1.916	.120
	365.4	53.0	18	61.0	11.13	-.428	2.182	.109	11.001	.195	-.703	2.457	.111
	313.7	45.5	18	127.6	21.23	.171	1.942	.141	11.743	.167	-.030	1.769	.147
0.44	334.4	48.5	18	53.6	15.47	1.667	4.833	0.272	10.857	0.238	1.210	3.899	0.214
	310.2	45.0	18	83.7	26.35	-.315	2.408	.067	11.277	.374	-1.091	3.747	.115
	289.5	42.0	18	142.6	41.59	.393	3.057	.148	11.825	.305	-.457	3.182	.118

[a]The Kolmogrov-Smirnov test rejection or acceptance is based on the absolute value comparison of maximum D with critical D given as follows:

Level of significance, α	Critical D value	
	n = 12	n = 18
0.01	0.338	0.278
.05	.375	.309

[b]Maximum D for normal distributions.

[c]Maximum D for log-normal distributions.

TABLE VIII. - LIFE DISTRIBUTION PARAMETERS FOR PHASE II RESULTS

[Sample size, 35.]

Stress ratio, $\bar{r}$	Alternating stress, S		Life, kilocycles		Skewness, α_3	Kurtosis, α_4	K-S test difference, D (a)	Chi-squared test		Life, $\log_e$ kilocycles		Skewness, α_3	Kurtosis, α_4	K-S test difference, D (a)	Chi-squared test	
	MN/m^2	ksi	$\bar{N}_f$	σ_{N_f}				Degrees of freedom	Value (b)	$\bar{N}_f$	σ_{N_f}				Degrees of freedom	Value (b)
			Normal distributions							Log-normal distributions						
∞	750.8	108.9	3 300	360	-0.163	2.317	0.094	1	0.248	8.095	0.112	-0.374	2.408	0.096	1	2.844
	634.9	92.1	6 400	610	-.325	1.672	.134	2	6.151	8.760	.097	-.402	1.684	.137	2	8.534
	507.4	73.6	14 200	1 370	-.447	2.654	.108	2	.880	9.554	.100	-.664	2.936	.128	1	.255
1.06	728.7	105.6	4 500	650	0.252	2.786	0.109	1	1.265	8.407	0.145	-0.141	2.991	0.087	1	0.288
	587.4	85.2	10 800	1 210	.200	2.187	.111	2	.726	9.281	.112	.016	2.089	.111	1	.728
	447.4	64.9	24 300	2 760	.757	2.095	.139	1	1.095	10.093	.110	.513	2.751	.117	2	1.595
	277.1	40.2	224 000	83 280	.650	3.143	.112	1	2.453	12.252	.380	.175	2.347	.114	2	8.188
0.40	342.6	49.7	59 000	9 610	0.969	3.626	0.154	1	3.029	10.973	0.155	0.567	3.126	0.122	0	(c)
	275.8	40.0	210 700	36 740	.735	3.364	.103	1	.631	12.244	.169	.313	2.722	.077	2	0.892
	242.0	35.1	332 700	110 670	1.478	5.138	[c] .201	1	2.928	12.670	.296	.682	3.237	.142	2	1.206
0.25	273.0	39.6	57 120	14 560	0.383	2.220	0.140	1	2.606	10.921	0.257	-0.075	2.352	0.094	2	2.862
	241.3	35.0	95 700	22 490	.597	2.790	.099	2	3.106	11.442	.231	.135	2.291	.068	2	.528
0.15	221.3	32.1	148 000	31 800	0.526	2.758	0.093	1	1.017	11.883	0.212	0.101	2.300	0.095	2	4.410
	188.9	27.4	272 100	64 500	.578	3.881	.106	1	3.875	12.487	.240	-.237	3.278	.086	1	3.011
	179.2	26.0	504 100	156 480	1.560	6.194	.194	0	(d)	13.091	.277	.722	3.272	[e] .147	1	1.226

[a]The critical diameter D_{cr} is 0.224 for a 0.05 level of significance and a sample size of 35.

[b]The accept or reject critical value for chi-squared test at 0.05 level of significance is 3.841 for 1 degree of freedom and 5.991 for two degrees of freedom.

[c]Maximum D for normal distributions.

[d]Not applicable.

[e]Maximum D for log-normal distributions.

TABLE IX. - ALTERNATOR ROTOR SHAFT DESIGN SUMMARY OF DESIGN BY RELIABILITY AND CONVENTIONAL DESIGN METHODOLOGIES

Parameter	Conventional design approach values	Design-by-reliability approach values
C_L	1.0	Not required
C_D	0.90	Not required
K_C	0.75	Not used
C_S	0.88	Not required
K_f	1.43	Not required
S'_n	644.6 MN/m^2 (93.5 ksi)	Not required
$S_{n,\,corr}$	268.9 MN/m^2 (39.0 ksi)	Not required
T	113 N-m (1000 lb-in.)	[a](112; 9) N-m (1000; 80 lb-in.)
M	14.1 m-N (126 in.-lb)	(14.1; 1.58) m-N (126; 11.4 in.-lb)
s_a	$\frac{144}{\bar{d}^3}$ MN/m^2 $\left[\frac{1.28}{\bar{d}^3}\right.$ ksi$\left.\right]$	$\left[\frac{144.}{\bar{d}^3};\ \frac{14.7}{\bar{d}^3}\right]$ MN/m^2 $\left[\frac{1.28}{\bar{d}^3};\ \frac{0.13}{\bar{d}^3}\right.$ ksi$\left.\right]$
s_m	$\frac{998}{\bar{d}^3}$ MN/m^2 $\left[\frac{8.83}{\bar{d}^3}\right.$ ksi$\left.\right]$	$\left[\frac{998.}{\bar{d}^3};\ \frac{91.5}{\bar{d}^3}\right]$ MN/m^2 $\left[\frac{8.83}{\bar{d}^3}\ \frac{0.81}{\bar{d}^3}\right.$ ksi$\left.\right]$
S_a	109.6 MN/m^2 (15.9 ksi)	[b](1213.3; 46.4) MN/m^2 (176.0; 6.73 ksi)
S_m	762.5 MN/m^2 (110.6 ksi)	
d	1.39 cm (35/64 in.)	1.07 cm (27/64 in.)
$\mathscr{R}$	(c)	0.999

[a]Normal distribution notation (mean; standard deviation).

[b]These are the parameters of the failure governing strength distribution $f(S_f)$ along $\bar{r} = 0.144$.

[c]The reliability obtained by the approach of Shigley (ref. 16, p. 169) is not theoretically applicable to this complex case; hence, the reliability is really not known for the conventional methodology.

TABLE X. - ALGEBRA OF NORMAL FUNCTIONS SUMMARY

[The expressions for mean and standard deviation for sums of differences of normal variates are exact. The remainder of the expressions are approximate only, and they are good approximations when the coefficient of variation V, of x and y are small, i. e., $V_x = (\sigma_x/\mu_x) < 0.10$ and $V_y = (\sigma_y/\mu_y) < 0.10$.]

Operation, z	Mean, μ_z	Standard deviation, σ_z (a)
Addition[b]: $z = x + y$	$\mu_x + \mu_y$	$\left(\sigma_x^2 + \sigma_y^2\right)^{1/2}$ or $\left(\sigma_x^2 + \sigma_y^2 + 2\rho\sigma_x\sigma_y\right)^{1/2}$
Subtraction[b]: $z = x - y$	$\mu_x - \mu_y$	$\left(\sigma_x^2 + \sigma_y^2\right)^{1/2}$ or $\left(\sigma_x^2 + \sigma_y^2 - 2\rho\sigma_x\sigma_y\right)^{1/2}$
Product: $z = xy$	$\mu_x\mu_y$ or $\mu_x\mu_y + \rho\sigma_x\sigma_y$	$\left(\mu_x^2\sigma_y^2 + \mu_y^2\sigma_x^2 + 2\rho\mu_x\mu_y\sigma_x\sigma_y\right)^{1/2}$ or $\left[\left(\mu_x^2\sigma_y^2 + \mu_y^2\sigma_x^2 + \sigma_x^2\sigma_y^2\right)(1 + \rho^2)\right]^{1/2}$
Quotient: $z = \frac{x}{y}$	$\frac{\mu_x}{\mu_y}$ or $\frac{\mu_x}{\mu_y} + \frac{\sigma_y^2\mu_x}{\mu_y^3}$ or $\frac{\mu_x}{\mu_y} + \frac{\sigma_y\mu_x}{\mu_y^2}\left(\frac{\sigma_y}{\mu_y} - \rho\frac{\sigma_x}{\mu_x}\right)$	$\frac{1}{\mu_y}\left(\frac{\mu_x^2\sigma_y^2 + \mu_y^2\sigma_x^2}{\mu_y^2 + \sigma_y^2}\right)^{1/2}$ or $\frac{\mu_x}{\mu_y}\left(\frac{\sigma_x^2}{\mu_x^2} + \frac{\sigma_y^2}{\mu_y^2} - 2\rho\frac{\sigma_x\sigma_y}{\mu_x\mu_y}\right)^{1/2}$
Exponent: $z = x^2$	μ_x^2 or $\mu_x^2 + \sigma_x^2$	$2\mu_x\sigma_x$ or $\left(4\mu_x^2\sigma_x^2 + 2\sigma_x^4\right)^{1/2}$
$z = x^3$	μ_x^3 or $\mu_x^3 + 3\sigma_x^2\mu_x$	$3\mu_x^2\sigma_x$ or $\left(3\sigma_x^6 + 8\sigma_x^4\mu_x^2 + 5\sigma_x^2\mu_x^4\right)^{1/2}$
$z = x^n$	μ_x^n	$n\mu_x^{n-1}\sigma_x$
$z = x^{1/2}$	$\left(\frac{1}{2}\sqrt{4\mu_x^2 - 2\sigma_x^2}\right)^{1/2}$	$\left(\mu_x - \frac{1}{2}\sqrt{4\mu_x^2 - 2\sigma_x^2}\right)^{1/2}$

[a] ρ = correlation coefficient. For completely uncorrelated variables, $\rho = 0$.

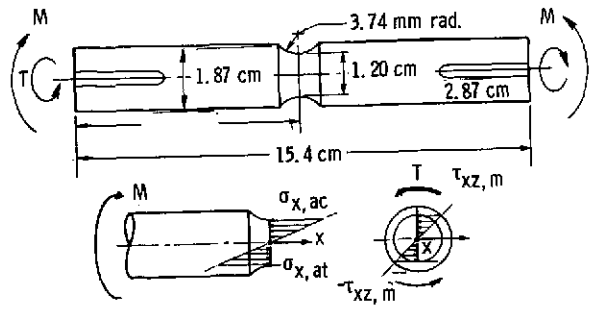

(a) Dimensions, finish, forces, and stresses.

(b) Before and after tests.

Figure 1. - Phase I specimen geometry. CS-60780

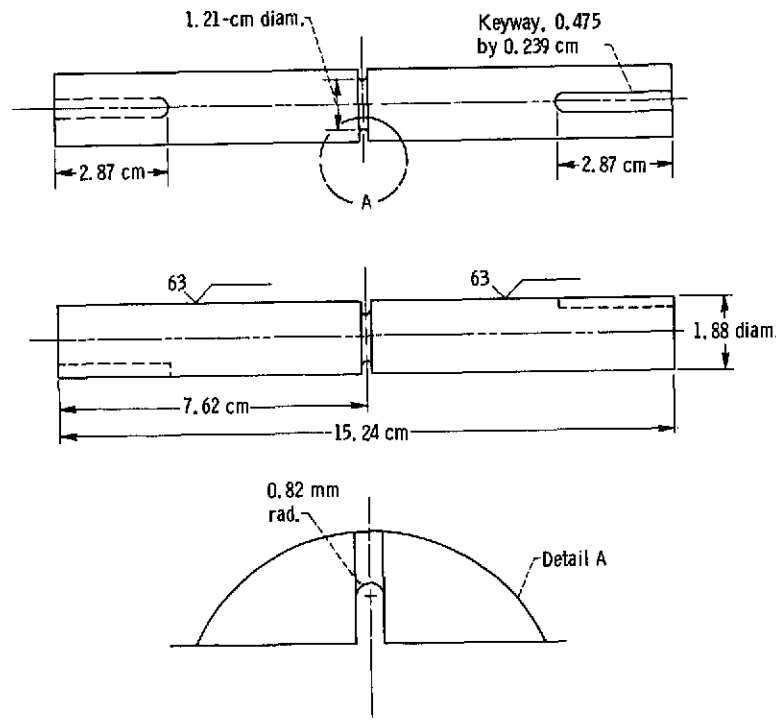

Figure 2. - Phase II research specimen geometry.

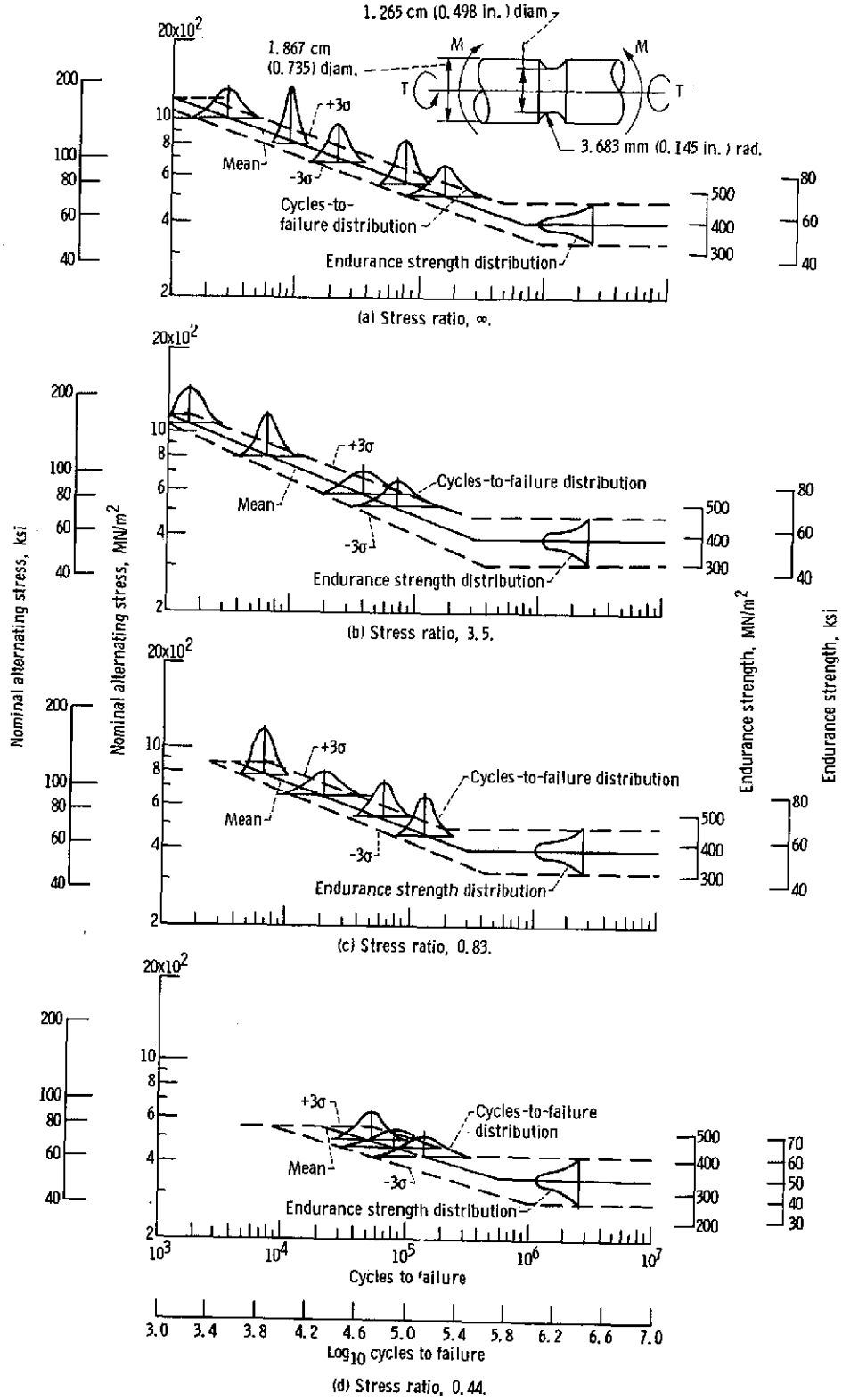

Figure 3. - Cycles-to-failure distributions of AISI 4340 steel; Rockwell C 35 to 40, phase I grooved specimens.

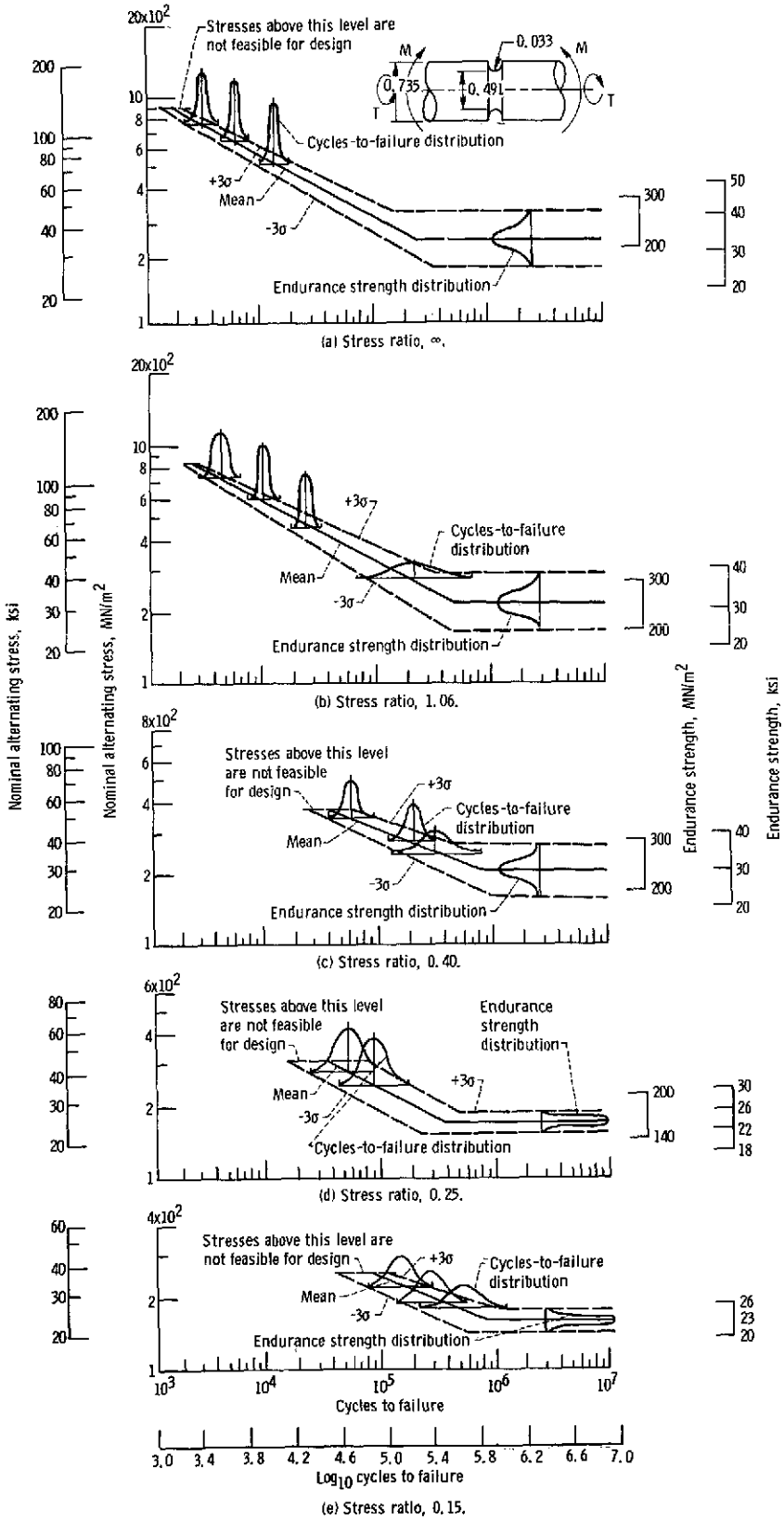

Figure 4. - Cycles-to-failure distributions. AISI 4340 steel, R_c 35 to 40 steel grooved specimens.

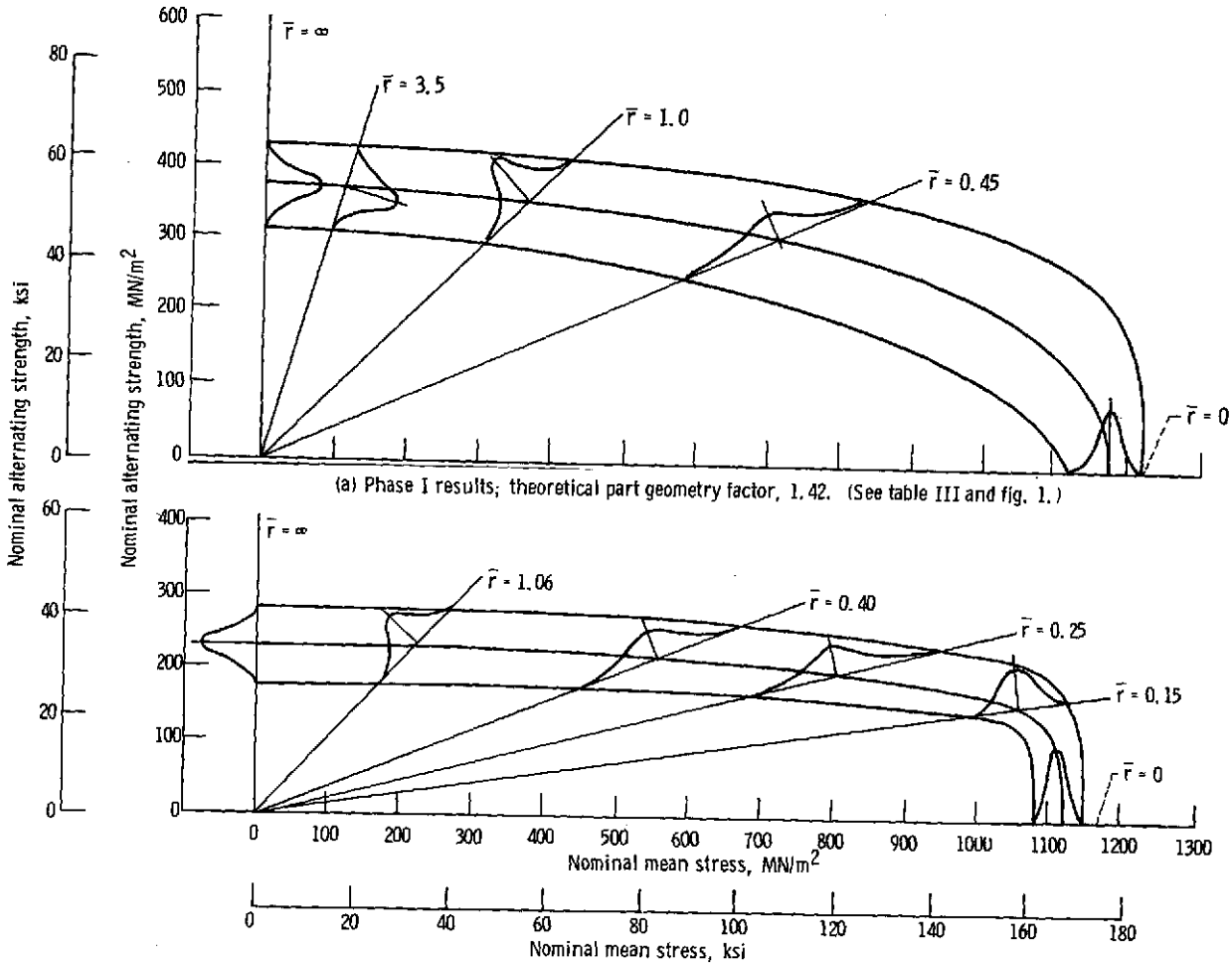

(a) Phase I results; theoretical part geometry factor, 1.42. (See table III and fig. 1.)

(b) Phase II results; theoretical part geometry factor, 2.34. (See table IV and fig. 2.)

Figure 5. - Distributional Goodman strength diagram. 2.5×10^6 Cycles of life; AISI 4340 steel; Rockwell C hardness, 35 to 40.

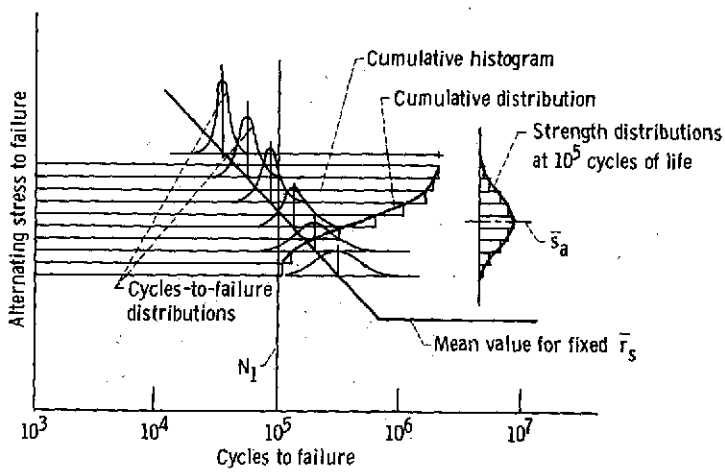

Figure 6. - Cumulative stress-to-failure distribution to strength distribution conversion technique.

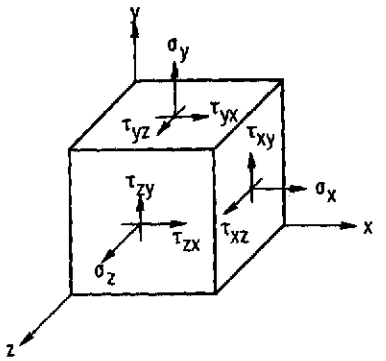

(a) xyz elements for volume.

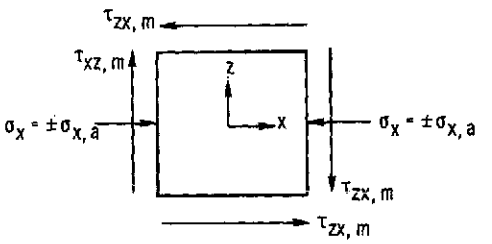

(b) x-z elements at surface.

Figure 7. - Rotating shaft stresses.

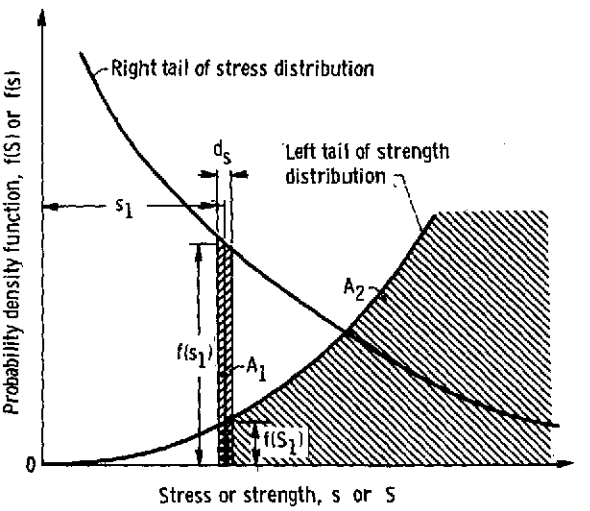

Figure 8. - Overlap region of stress into strength.

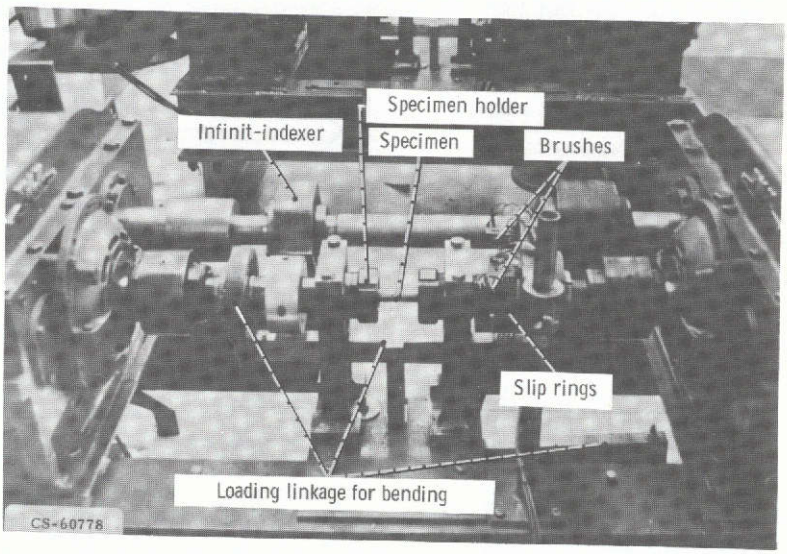

Figure 9. - Closeup of combined-stress - fatigue research machine.

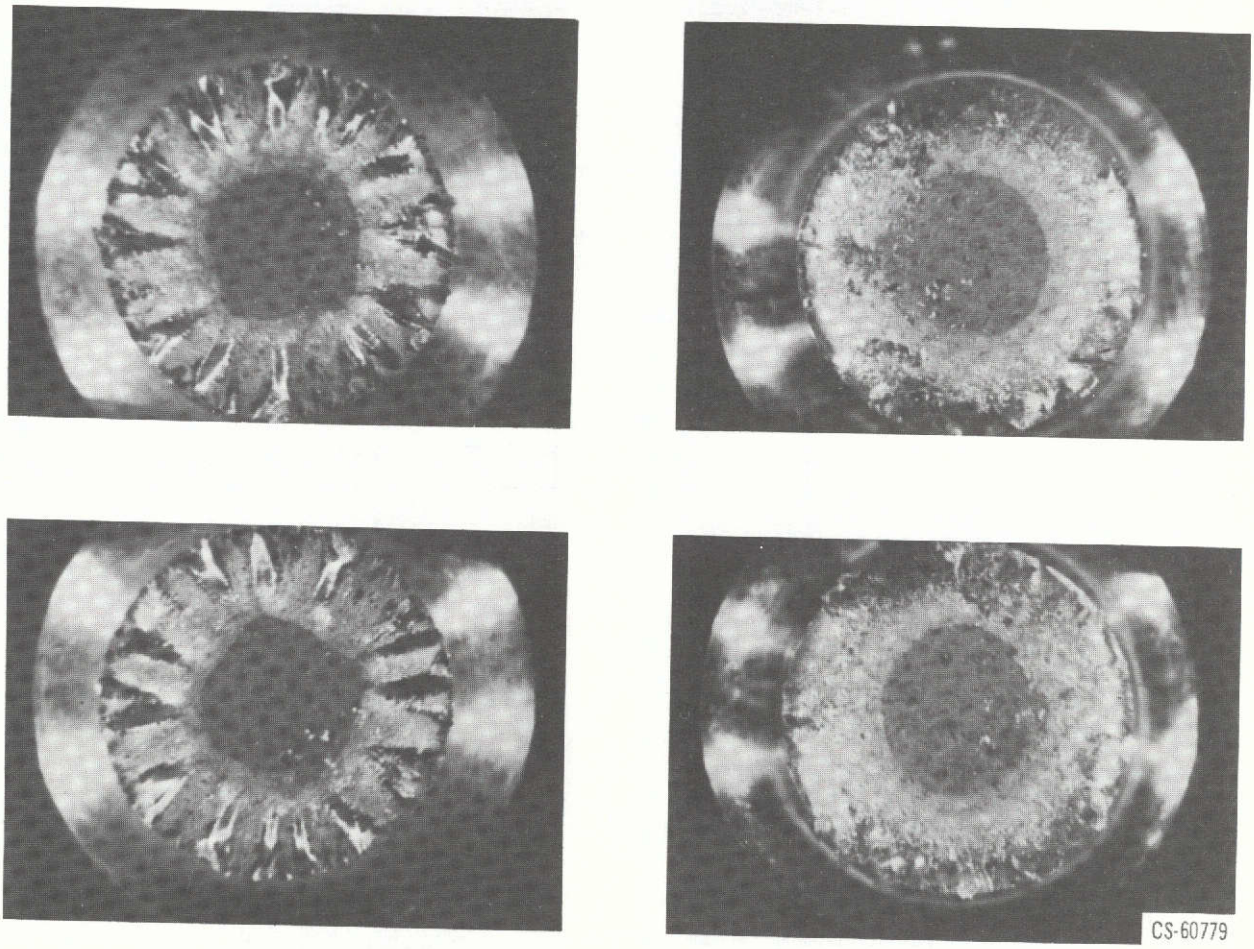

(a) Stress ratio, 0.83; alternating bending stress, 770 MN/m^2 (111.7 ksi); mean shear stress, 534 MN/m^2 (77.5 ksi).

(b) Stress ratio, ∞; alternating bending stress, 790 MN/m^2 (114.6 ksi); mean shear stress, 0.

Figure 10. - Closeup of fractured section at notch.

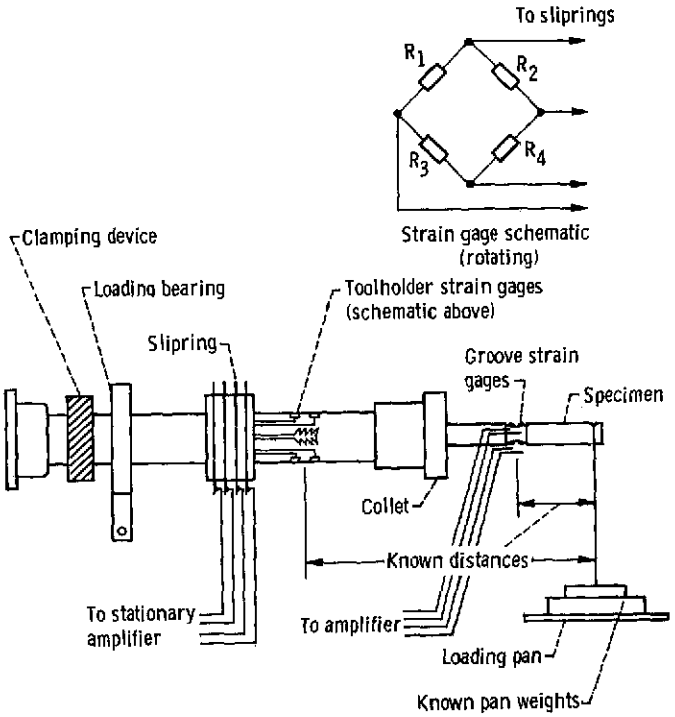

Figure 11. - Test setup for bending calibration.

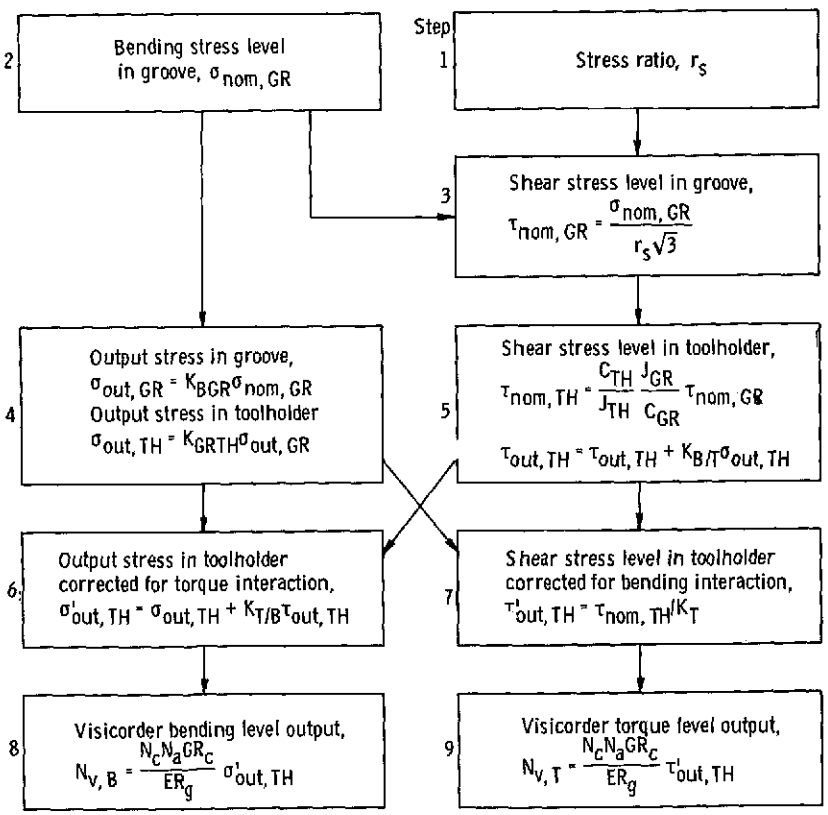

Figure 12. - Calibration flow chart showing use of calibration results given in table IV to assure proper specimen environment.

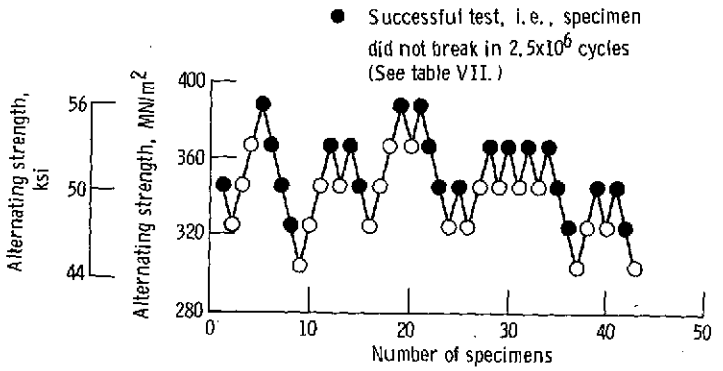

Figure 13. - Endurance strength data. Stress ratio, 0.44; SAE 4340 steel; Rockwell C hardness, 35 to 40; grooved specimens.

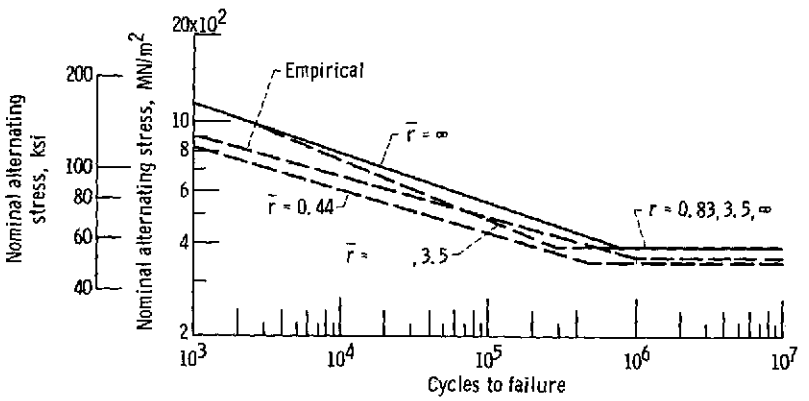

Figure 14. - Experimental and empirical S-N diagrams based on phase I results.

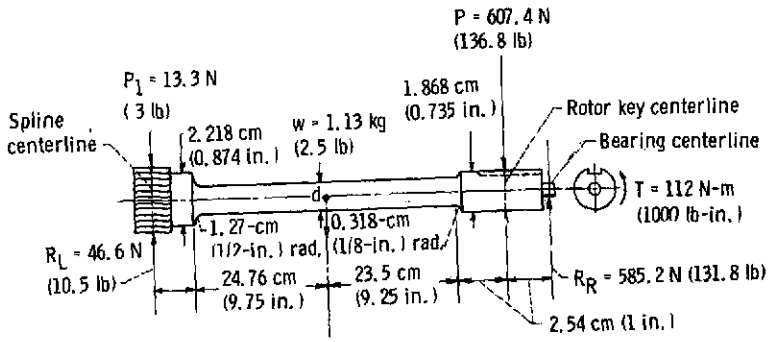

(a) Inner shaft details.

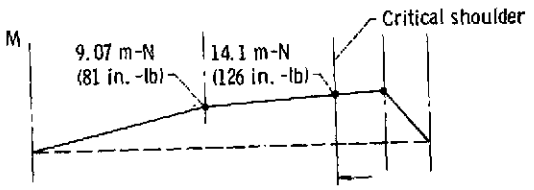

(b) Bending moment diagram.

Figure 15. - Alternator inner rotor shaft.

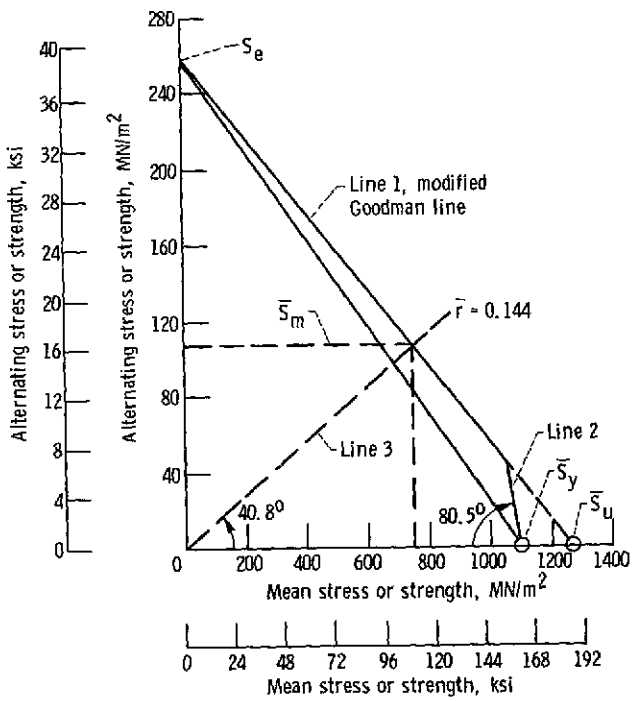

Figure 16. - Conventional combined-stress fatigue diagram showing modified Goodman line, Soderberg line, and stress ratio line for deterministic shaft design example.